FixI1 and FixI2:
Homologous Proteins with
Unique Functions in
Sinorhizobium meliloti

by

Jessica Collins

A Thesis
Submitted to the Faculty of

WORCESTER POLYTECHNIC INSTITUTE
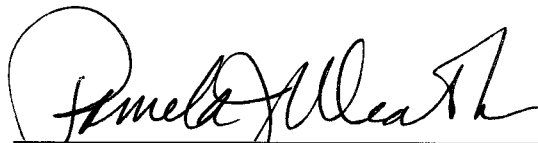
in partial fulfillment of the requirements for the

Degree of Master of Science
in Biochemistry

March 2014

APPROVED:

_____
Dr. Jose Argüello,
Advisor

_____
Dr. Pamela Weathers,
Committee Member

_____
Dr. Arne Gericke,
Department Head

_____
Dr. Robert Dempski,
Committee Member

TABLE OF CONTENTS

ABSTRACT

Cu^+-ATPases are transmembrane enzymes that couple the efflux of cytoplasmic Cu^+ to the hydrolysis of ATP. It is well established that Cu^+-ATPases control cytoplasmic Cu^+ levels. However, bacterial genomes, particularly those of symbiotic/pathogenic organisms, contain multiple copies of genes encoding Cu^+-ATPases, challenging the idea of a singular role for these enzymes. Our lab has demonstrated that one of the two Cu+-ATPases in *Pseudomonas aeruginosa,* a FixI-type ATPase, has an alternative role, most likely Cu^+ loading of cytochrome c oxidase (Cox). To further study alternative roles of Cu^+-ATPases, we study the symbiont *Sinorhizobium meliloti*. Rhizobia are soil-dwelling bacteria that interact with legumes, forming plant root nodules that actively fix N_2. The *S. meliloti* genome contains five Cu^+-ATPases, two of which are FixI-type. Both of these enzymes, termed FixI1 and FixI2, are downstream of Cox operons. We hypothesized that the presence of multiple FixI-type ATPases was not an example of redundancy, but rather is an evolutionary adaptation that allows rhizobia to survive under the wide variety of adverse conditions faced during early infection and establishment of symbiosis. Towards this goal, this work focused on examining the effects of mutation of each ATPase on both free-living bacteria and on the ability of rhizobia to establish an effective symbiosis with its host legume. Each of these mutants presents a different phenotype at varying points of the nodulation process, and only the *fixI2* mutation produces a respiratory-deficient phenotype during aerobic growth. These results are consistent with our hypothesis that the two proteins have non-redundant physiological functions. Understanding the factors that contribute to an effective symbiosis is beneficial, since N_2 fixation in legumes is important to both agriculture and industry.

LIST OF FIGURES

List of Tables

Appendix

ACKNOWLEDGEMENTS

I would like to thank Dr. Daniel Raimunda, Dr. Aniruhda Dixit, and Evren Kocabaş, for their contributions to this work and invaluable discussions. I am also grateful to my fellow graduate student, Sarju Patel, for all of your help and support. I wish you all the luck in your PhD!

I would especially like to thank Dr. Teresita Padilla Benavides, for her guidance and support during the course of this work, for all of her contributions to the experiments described in this report, and especially for all the beers, wine and food. I consider myself so, so lucky to have worked with you. Te amo.

I also gratefully acknowledge Courtney McCann, not only for her hard work in generating the CopA-CopZ interaction model, but also for always giving me a reason to laugh.

I am grateful to the entire CBC department—faculty, postdocs, and fellow grad students. You have all been so supportive during the past few years, and I could not have asked for a better group of colleagues. Thank you all.

I would also like to thank my parents for their unwavering support, and my children for their understanding and cooperation during long nights in the lab. I will never understand how racking pipette tips can keep a 5 year old entertained for so long, or why pelleting and washing cells is so fascinating, but thankfully, it was.

I would also like to thank Dr. Rob Dempski and Dr. Pam Weathers for taking the time to be part of my Thesis Committee.

And, last but certainly not least, I thank my advisor, Dr. José Argüello, for his guidance, advice, and patience. My time in your lab changed my life. I will forever be grateful to you for giving me that opportunity.

1. INTRODUCTION

The importance of transition metal homeostasis during host-pathogen interaction is becoming increasingly evident. The presence of multiple copies of a specific type of metal-specific efflux transporter, known as the P-type ATPase, in the genomes of pathogenic/symbiotic bacteria strongly suggests that each of these transporters plays a specific alternative physiological role during interaction with the host (1). The focus of this project was to identify distinct physiological roles of two of the five Cu^+-ATPases present in the genome of *Sinorhizobium meliloti*, FixI1 and FixI2.

1.1 Metals in biology

Approximately one-third of all enzymes require a metal co-factor for proper structure or function (2). Among these are diverse classes of molecules functioning in roles involved in cellular respiration, such as cytochrome *c* oxidase (Cox), oxidative stress mediation, such as the Fe/Mn-superoxide dismutase (SOD) and the Cu/Zn-SOD, and in regulation of gene expression, such as zinc-finger transcription factors (3). Thus, in biological systems transition metals play essential roles as metal micronutrients. Because of the diverse functions of the metalloenzymes present in the cell, the cell must maintain a proper quota of biologically relevant metals. Dietary and/or metabolic metal deficiencies can cause a number of pathological conditions in humans (4-6). Sufficient cellular metal levels are also important in bacteria, particularly in host-pathogen interactions (see below)(2).

However, levels of bioavailable metals in the cytoplasm must be tightly regulated lest they become toxic (7). In excess, many metals are able to participate in Fenton chemistry, where the reduced metal ion catalyzes the activation of oxygen from hydrogen peroxide (8). This activated oxygen can then generate free radicals and reactive oxygen species (ROS), which in turn damage cellular biological targets such as DNA, protein, and lipids (8). Additionally, metals can directly interact with oxygen, nitrogen, and sulfur moieties present in amino acid side chains, and oxidize histidine, proline, lysine, methionine, and cysteine residues in proteins (9). In particular, increases in cytoplasmic Cu^+ levels have a deleterious effect, as this metal also disrupts iron-sulfur clusters (10). For this reason, Cu^+ levels in cells are tightly regulated by various homeostatic mechanisms (11, 12), resulting in the virtual absence of free Cu^+ in the cytoplasm (13).

Chief among the mechanisms by which cells regulate the proper distribution of metals are metal specific efflux transporters, including members of the P-type ATPase superfamily (14) and the resistance-nodulation-division (RND) superfamily of transporters (15). Both are membrane proteins that couple the efflux of metals to either the hydrolysis of ATP or to proton transport. Cells also maintain metal homeostasis through the action of the metal-responsive transcription factor (TF) (11, 16). These TFs regulate genes by one of two main mechanisms. Under metal starvation conditions, some TFs, such as CsoR in *Mycobacterium tuberculosis*, act to increase expression of metal-specific importers and/or decrease expression of metal efflux proteins (17). Under conditions of metal excess, other TFs like ZitR in *Escherichia coli*, induce the expression of efflux transporters such as P-ATPases (18), as well as other molecules that can act to sequester the metal, such as metallochaperones and metallothioneins.

1.1.1 Copper homeostasis systems in bacteria

Two bacterial model systems have been used to study intracellular copper homeostasis: *E. coli* and *Enterococcus hirae* (12, 19). Both species contain three known cuprohomeostatic systems, all of which regulate Cu^+ efflux from the cell. The mechanisms that control copper influx in bacterial systems have not yet been described. Because of the potential for Fenton chemistry and other deleterious effects, the intracellular level of copper must be tightly controlled, and virtually all cytoplasmic copper is bound with high affinity to chelators and chaperones (13). This results in virtually undetectable levels of free copper in the cell, with the overall cellular copper levels being in the 10-100 μM range (13, 20). Despite lack of experimental evidence about copper import or regulatory elements that control the rate of uptake, the ability of the cell to sequester virtually all free Cu^+ from the cytoplasm creates a high concentration gradient that is likely a driving force behind influx.

The efflux of copper in bacteria is regulated by at least one of three different homeostatic systems: the Cue (copper efflux) operon, which encodes a P-type ATPase and is regulated by the metal-responsive transcription factor CueR (21); the PcoABCD system, regulated by the two-component regulatory system PcoRS (22); and the CusCFBA (copper-sensing) system, which is regulated by the two-component regulatory system CusRS (Fig. 1) (23). Recent phylogenomic approaches have found that all
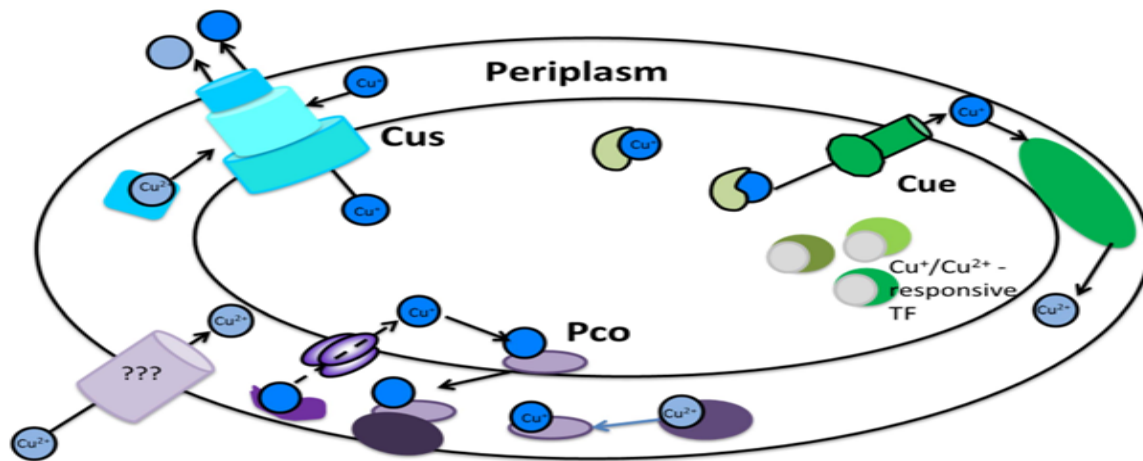
Figure 1: The three main Cu$^+$ regulating systems in bacteria. The Cue system is responsible for maintenance of cytoplasmic Cu$^+$ levels, while the Pco system protects against Cu$^+$ stress in the periplasm. The Cus system appears to accept Cu$^+$ from both the cytoplasm and the periplasm.

bacterial species examined contain at least one Cue system; however, the presence of the PcoABCD and CusCFBA systems is not ubiquitous (24). This observation is consistent with the roles of each of these systems: the Cue system is a chromosomally-encoded system responsible for efflux of Cu$^+$ from the cytosol, whereas the PcoABCD system is encoded on a plasmid and protects against Cu^{2+} stress in the periplasm (22). The role of the CusCFBA, system, which is also encoded in a plasmid, is less clear; experimental evidence suggests that this system is able to secrete both Cu$^+$ from the cytoplasm and Cu^{2+} from the periplasm (23).

The ubiquitous Cue system has two main components: CopA (also termed CtpA, ActP, CtpV), a Cu$^+$-ATPase, and CueO, a multi-copper oxidase having laccase-like activity (25). The Cue operon often contains a cytosolic Cu$^+$ chaperone such as CopZ (26, 27). Transcription of the operon is regulated by a metal-responsive TF, CueR, which is activated by elevated levels of either Cu$^+$ or Ag$^+$ in the cytoplasm. The *copA* mutation results in a well-described Cu$^+$-sensitive phenotype (26-29). The CueO protein has been implicated with copper tolerance; each CueO monomer binds four Cu$^+$ atoms and contains a Tat secretion signal that localizes the protein to the periplasm (30, 31). It is unlikely that copper tolerance is provided by translocation of Cu$^+$ to the periplasm by CueO, as CopA performs this function far more efficiently. Rather, CueO is thought to have a protective function by sequestering Cu$^+$ in the cytoplasm and oxidizing periplasmic Cu$^+$ ions to the less-toxic Cu^{2+} (25). In general, Cu$^+$ is transported out of the cytoplasm in the reduced form. However, the existence of some Cu^{2+}-ATPases, such as

Archaeglobus fulgidus CopB, indicates that in some species, the metal is present in the cytoplasm in both redox states (32).

Some strains of bacteria encode Cu$^+$ resistance operons in plasmids that allow them to survive at much higher copper concentrations than the Cue system would allow (33). One example is the *pcoABCD* operon, which is regulated by the PcoRS proteins. These proteins constitute a two-component regulatory system responsible for sensing periplasmic Cu^{2+} levels (Fig. 2) (34). PcoA, like CueO, also binds Cu$^+$ in the cytoplasm and is secreted by the Tat pathway, and is able to functionally replace CueO in *E. coli* (22). PcoB and PcoD are outer and inner membrane proteins, respectively. PcoC is localized to the periplasm, and is thought to deliver Cu$^+$ to PcoD. Another gene, *pcoE,* is also required to confer copper resistance. The expression of PcoE results in an increase of periplasmic copper levels, suggesting the protein plays a role in periplasmic binding, possibly as a chaperone delivering Cu$^+$ to PcoA (22). However, PcoE expression is regulated by the CusRS two-component regulatory system, and thus is not part of the *pco* operon (35).
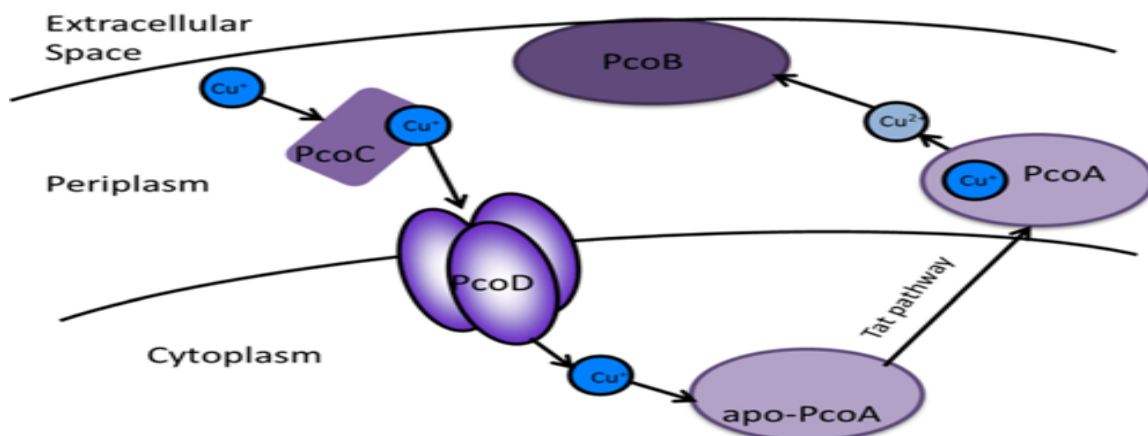
Figure 2: Putative organization of the PcoABCD system. PcoA is thought to bind Cu+ in the cytoplasm, reduce it to Cu2+ in the periplasm, and deliver it to PcoB, an outer membrane protein. PcoC binds Cu+ and delivers it to PcoD, an inner-membrane protein, for delivery to apo-PcoA.
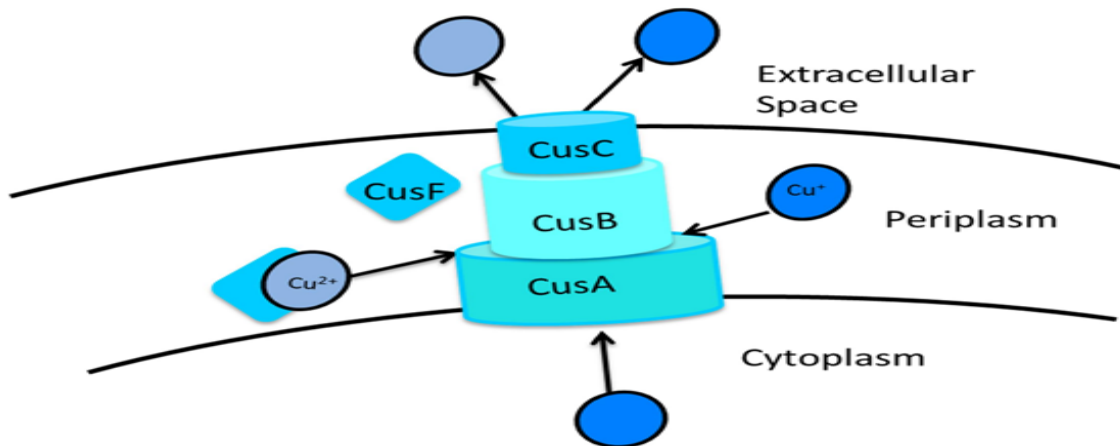
Figure 3: Putative organization of the CusCFBA system. The soluble periplasmic protein Cus B is thought to bridge CusA and CusC, which are localized to the inner and outer plasma membranes, respectively. CusF is a soluble periplasmic chaperone that can deliver Cu^{2+} to Cus A for efflex. Conversely, CusA can also transport Cu^+ from either the cytosol or from the periplasm.

Another example is the *cusCFBA* operon, which encodes a tripartate-transport system. Experimental evidence suggests it transports Cu^+ from both the periplasm and the cytoplasm out of the cell across the outer membrane (15, 35, 36). The Cus complex consists of four proteins (Fig. 3): CusA, an inner membrane pump; CusB, a periplasmic protein; CusC, and outer membrane protein; and CusF, a copper-binding protein. CusA is an RND-type protein that putatively transports Cu^+ from the cytoplasm to the periplasm (36). The CusB protein is thought to interact with both CusA and CusC simultaneously, bridging the two proteins to form a channel. In this way, Cu^+ might be pumped directly from the cytoplasm through Cus A to the extracellular milieu through CusC (37). Alternatively, CusF delivers Cu^+ to CusB (38). The expression of the *cusCFBA* operon is induced by the presence of Cu^+, but it is important to note that deletion of *cusCFBA* does not show the Cu^+ sensitive phenotype of the *copA* mutation. A *copA-cusCFBA* double mutant was no more sensitive to Cu^+ than the *copA* mutant, providing further evidence that CusCFBA is mainly responsible for periplasmic, not cytoplasmic, Cu^+ levels (23).

1.1.2 Role of metals in host-pathogen interactions

The dual nature of metals as both essential micronutrient and potential toxin plays a central role during the host-pathogen interaction (39). Upon infection, a host cell responds by the sequestration of Fe and Mn. This effectively "starves" the invading bacteria of essential metal nutrients (40). Another typical host response is "flooding" the macrophage with toxic levels of metals, such as Cu^+ and Zn^{2+} (41, 42). Thus, in order for

the pathogen to survive, it must be able to scavenge for scarce metals via siderophores, as well as sequester or secrete excess metals from the cytoplasm. Additionally, invading bacteria can produce enzymes to help mediate the stress produced by high metal levels (e.g., ROS produced via Fenton chemistry). Most of these enzymes, including, catalases, Cox, and SODs, require a metal cofactor.

1.2 P-type ATPases

P-type ATPases (P-ATPases) are polytopic membrane proteins that function to transport a variety of substrates against electrochemical gradients. This transport is achieved by coupling the transport to the hydrolysis of ATP. Some members of this family, such as the Na^+, K^+-ATPase, the sarcoplasmic reticulum Ca^{2+}-ATPase, and the gastric H^+,K^+-ATPase, have been extensively characterized. These enzymes all follow the classical Post-Albers E1/E2 catalytic cycle (Fig. 4) (43). A unifying characteristic belonging to all P-ATPases is a conserved DKTGT sequence; this aspartyl residue is the site of catalytic phosphorylation required for transport (44).
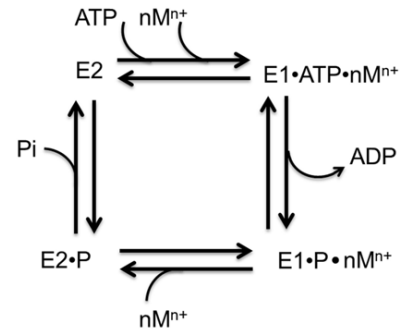
Figure 4: Generalized E1/E2 catalytic cycle. The E1 conformation is formed upon binding of metal and ATP. Hydrolysis of ATP results in release of ADP and a metal-bound phospho-enzyme. Release of metal ions, and subsequently Pi, regenerates the E2 conformation.
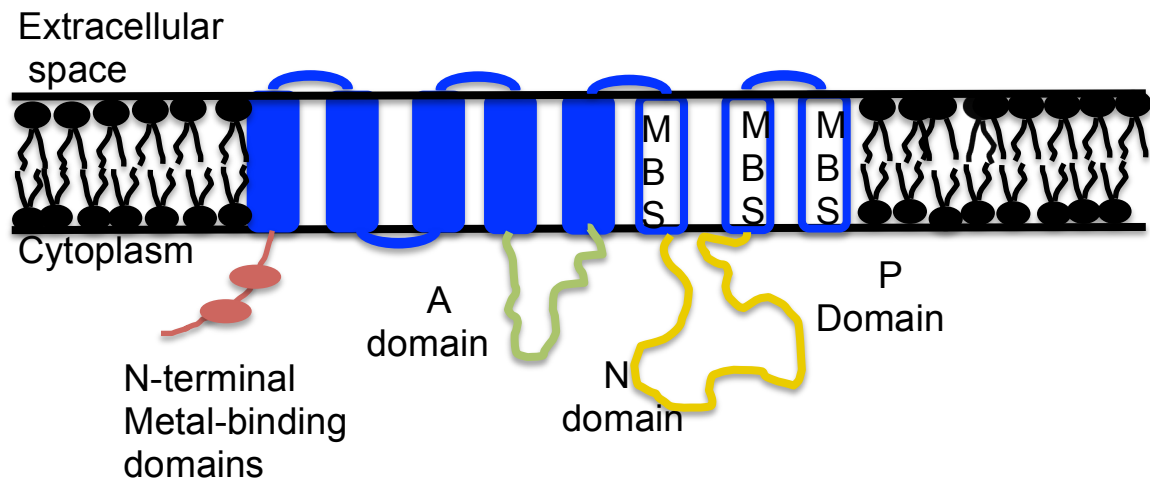
Figure 5: Schematic of the Cu$^+$-ATPase structure, highlighting characteristics common to all P-type ATPases. All contain a core catalytic structure consisting of 6 TM helices, and cytosolic actuator, nucleotide-binding, and phosphorylation domains, labeled A (green), N, and P (both yellow) above. The last three helices of the TM core contain subfamily-specific residues that constitute metal-binding sites (MBS), which determine substrate specificity.

The P-ATPase superfamily can be subdivided into five distinct subfamilies (P1-P5). All P-ATPases, regardless of subfamily, share multiple conserved domains (Fig. 5) (14). The major criterion for P-ATPase subgroupings is the total number and arrangement of their transmembrane (TM) helices. Subfamilies are then further arranged into subgroups based upon conserved signature sequences in the TM regions, which determine substrate specificity (45).

The P_1-ATPase family is composed the P_{1A}-type ATPases, which are part of the prokaryotic K^+ transport system, and the P_{1B}-type ATPases, which transport transition metals in all organisms. The P_2-type ATPase family is a very-well characterized group that consists of the eukaryotic endoplasmic reticulum (ER) and the sarcoplasmic reticulum (SR) Ca^{2+}-ATPases; rarely, Ca^{2+}-ATPases are present in the prokaryotic inner membrane. The Na^+, K^+-ATPase and the H^+,K^+-ATPase are also members of the P_2-ATPase family. The P_3-ATPase family consists of a group of plasma membrane (PM) proton ATPases unique to fungi and plants. Both the P_4 and P_5-ATPases are present only in eukaryotes (1). The P_4-ATPases, also referred to as "flippases," are responsible for transport of phospholipids from one leaflet of the PM to the other (46). The substrate(s) of the P_5-ATPases are unknown (14).

1.2.1 Structural Features of P_{1B}-type ATPases

Structurally, all members of the P-ATPase family share three conserved cytoplasmic domains: the phosphorylation (P-domain), the actuator (A-domain), and nucleotide-binding (N-domain) (Fig. 5) (14). Additionally, many of the P_{1B}-ATPases contain cytoplasmic regulatory metal-binding domains (MBD) in the N-terminus, C-terminus (N-MBDs and C-MBDs, respectively), or both (47, 48). These domains do not participate in metal transference to the TM-MBS, but rather control the rate of enzyme turnover, most likely through interactions with a cytoplasmic loop (49, 50). A key feature of the P_{1B}-ATPase is the presence of conserved amino acids in the TM region (1). Specific residues associated with particular metal specificities will be discussed later.

1.2.2 Catalytic Domains

The A-domain is connected to the TM regions of the protein by long, flexible linker sequences, which allow the domain to move and rotate during the catalytic cycle (51). This rotation allows a consensus sequence, TGE, to move up toward the bound

ATP. A water molecule coordinated between the conserved E residue and the phosphorylated D and acts as a nucleophile, attacking the phosphate bond and catalyzing dephosphorylation.

The P-domain is the most highly conserved of these domains, and is the site of enzyme phosphorylation (14). The N-domain is responsible for ATP binding and is connected to the P-domain by a narrow hinge (52). The specific residues involved in ATP binding are not conserved across families, making the N-domain the most variable of the three catalytic domains. Together, the P- and the N-domain are referred to as the ATP-binding domain. Regardless of the specific residues present at the ATP-binding site, all make contact with only the adenosine (14).

1.2.3 Transmembrane Binding Sites in P_{1B}-type ATPases

The P_{1B}-type ATPases are divided into subgroups based upon transported substrate. Substrate specificity is determined by the TM region of the enzyme, both by the number and distribution of the TMs present and by conservation of particular residues in key TM helices (1). Structural-functional studies of Cu^+, Cu^{2+}, Co^{2+} and Zn^{2+}-ATPases, for example, have made it possible to determine which residues are responsible for binding during transport (1). This identification of TM-MBS allows the prediction of metal specificity of P_{1B}-ATPases based upon sequence alone (Table 1).

Subfamily	Specificity	TM 4	TM 5	TM 6
P_{1B-1}	Cu^+	CPC	NYG	MXXS
P_{1B-2}	Zn^{2+}	CPC	H	D G
P_{1B-3}	Cu^{2+}	CPH	NYG	MSST
P_{1B-4}	$Co^{2+}/Cu^{2+}/$ $Mn^{2+}/Zn^{2+}/$ Ni^{2+}	SPC		HEGT
P_{1B-5}	Ni^{2+}/Fe^{2+}	(T/S)PCP		QEXXD

Table 1: Conserved TM residues of P_{1B}–ATPase subfamilies. Each subfamily has a unique, consensus sequence of amino acids constituting the TM-MBS, which is the determinant of physiological substrate metal ion specificity.

Although these residues can be used to predict physiological substrates, it should be noted that physical and chemical similarities between metal cations can lead to ATPase activation and transport of non-physiological substrates. For instance, the Cu^+-ATPase can also be activated by Au^+ and Ag^+ (53); Zn^{2+}-ATPases can be activated by Cd^{2+} and Pb^{2+} (54, 55); and P_{1B-4}-ATPases have been shown to transport Co^{2+}, Cu^+, Zn^{2+}, Mn^{2+} and Ni^{2+} (56-59).

The major determinant of metal binding to particular residues lies in the residues constituting the TM-MBS. The P_{1B1}-ATPases are Cu^+ efflux transporters, and are the best characterized group of P_{1B}-type ATPases. This subgroup consists of at least two different types of enzymes: the classical CopA-type ATPases and the FixI/CopA2-like ATPase (60, 61). Though these two enzymes differ in both their affinity for Cu^+ and their respective turnover rates, they contain identical TM-MBSs that bind 2 Cu^+ ions with femtomolar affinity in a trigonal planar coordination formed by the invariant residues CXC in TM 6, NY in TM 7, and MXXS in TM 8 (60).

The P_{1B-2}-ATPases, the Zn^{2+} exporters, contain two C residues in TM 6, an H in TM 7, and D and G residues that constitute their TM-MBS (62). Members of the P_{1B-3}-ATPase family, which transport Cu^{2+}, have slightly different TM-MBS than the P_{1B-1}-ATPases: a CXH in TM 6, the same NY in TM 7, and an MSST motif in TM 8 (32). The differences in these metal-binding sites favor a tetrahedral coordination, the preferred coordination chemistry for the borderline Lewis acid Cu^{2+} (3). Additionally, the imidazole function of the H residue forms a stronger adduct with Cu^{2+} than with the soft Lewis acid Cu^+ (63).

The P_{1B-4} and P_{1B-5}-ATPases differ from the first three subgroups in that they contain only 6 TM helices and lack cytoplasmic MBDs (1). The P_{1B-4} –ATPase subgroup, which have been shown to transport Co^{2+}, Cu^{2+}, Mn^{2+} , Zn^{2+} , and Ni^{2+} , have only two conserved sequences: SPC in TM 4 and HEGT in TM 6 (1, 58). The P_{1B-5}-ATPases contain a conserved (T/S)PCP in TM 4 and a QEXXD sequence in TM6; substrate specificity has yet to be determined (1, 64).

1.2.4 Catalytic cycle of the Cu$^+$-ATPase

The high level of structural conservation amongst all members of the ATPase superfamily implies that they share a common pumping mechanism. Studies have shown that all P-ATPases follow the Post-Albers E1-E2 model (Fig. 4) (43, 65), which describes the enzyme as cycling between one of two enzyme conformations: the E1 conformation, which has high affinity TM-MBS oriented towards the cytoplasm, and the E2 conformation, which decreases the affinity of the TM-MBS and positions them so that the sites are exposed to the periplasm/extracellular space (14, 66). Using the SERCA catalytic cycle as an example, the highlights of the transport mechanism are as follows. Briefly, ions bind to the TM-MBS of the enzyme in the E1 conformation, causing a change in the conformation of the P-domain and allowing Mg^{2+}-ATP to bind the P- and N-domains, forming the E1-ATP state. Phosphorylation of the conserved aspartic acid causes further "bending" of the P-domain and generates the E1-P-ADP state (14, 66). This phosphorylation also induces a rotation in the A-domain through a flexible linker attached to TM 6, positioning the conserved TGE closer to the phosphorylated D residue, generating the E2-P state. This is the rate-limiting step of the catalytic cycle.

Once the enzyme has reached the E2-P state, the ions are now able to diffuse out of the now low-affinity TM-MBS and are released to the periplasm or extracellular space. In many cases, counterions bind to the TM-MBS, closing the exit pathway through the TM region and allowing the TGE of the A-domain to coordinate a water molecule. This water can then act as nucleophile and catalyzes the dephosphorylation of the ATPase and the release of phosphate and ADP. This allows the A- and P-domains to rotate back to their relaxed positions, regenerating the E1-state, completing the catalytic cycle (14).

Although the overall E1-E2 catalytic cycle provides a basic understanding of the mechanism of the P-ATPase, there are some major differences in the specific transport mechanism of Cu$^+$-ATPases (Fig. 6). In many classical P-ATPases, such as the Ca^{2+}-ATPases, ion(s) access the TM-MBS as "free" ions. However, due to the highly reactive nature of the Cu$^+$ ion, free Cu$^+$ does not exist in the cytoplasm, and only exists in the cytoplasm bound to sequestering proteins such as metallothioneins and copper chaperones (13). Thus, *in vivo*, copper chaperones, such as CopZ in *A. fulgidus*, are required for Cu$^+$ delivery to the TM-MBSs in CopA (67).
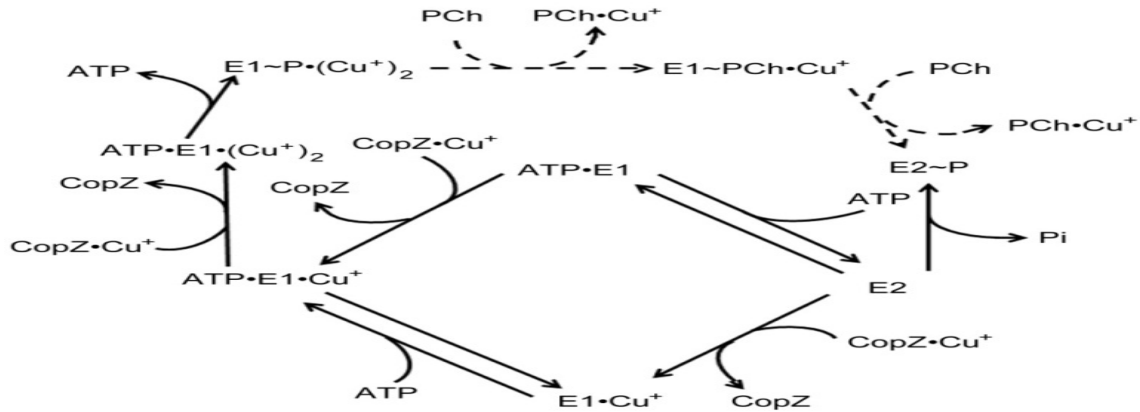
Figure 6: Catalytic and transport cycle of the Cu+-ATPase. Binding of two Cu+ atoms from the cytoplasm to the TM-MBSs of the E1 enzyme conformation is coupled to ATP hydrolysis. Note the irreversibility of Cu+ transfer from CopZ to the enzyme. Full occupancy of the TM-MBSs requires the presence of ATP. Enzyme phosphorylation causes a conformational change to theE2~P conformation, causing the TM-MBSs to open to the extracellular/periplasmic compartment and release of Cu ions. Enzyme dephosphorylation returns the ATPase to the E1conformation, with the TM-MBSs once again facing the cytoplasm. Dashed lines represent the hypothetical mechanism of Cu+ release to a periplasmic chaperone (PCh) or other metal acceptor in the periplasm.

Recent studies in our laboratory have focused on the mechanism of Cu^+ transfer from CopZ to CopA in *A. fulgidus* (67, 68). Our lab has demonstrated that the absence of the N-MBD does not affect the rate of Cu^+ transference from CopZ to CopA, indicating that the Cu^+ ion is directly transferred from CopZ to the TM-MBS of CopA (67). The crystal structure of LpCopA, the Cu^+ ATPase from *Legionella pneumophila* has given
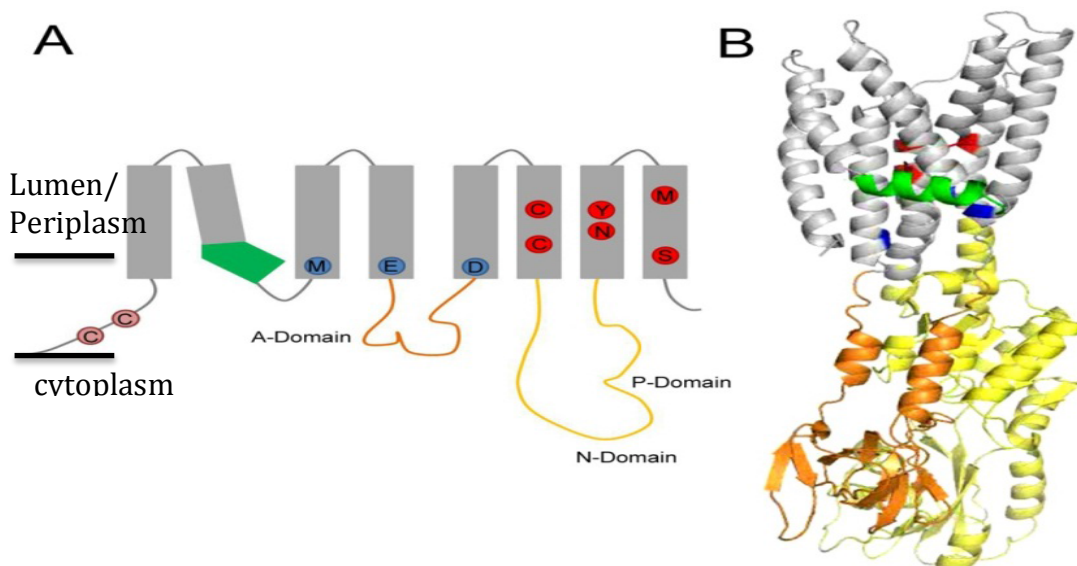
Figure 7: Structure of the Cu^+-ATPase. (A) Topology model highlighting the kinked helix comprising the CopZ docking site (green), Cu^+-entry site residues (blue), TM Cu^+-binding residues (red), and the A-and ATP-binding domains (orange and yellow, respectively). (b) The same features high- lighted in the topology model, transposed onto the crystal structure of *Legionella pneumophila* CopA (3RFU).

insight as to how this transference might occur (Fig. 7) (69). The crystal structure shows a "kinked" TM helix at a GG motif conserved amongst P_{1B1}-type ATPases (69). This kink is part of an ampipathic helix with positive residues (K, R, R, and R) that could interact with negative charges (four E residues) on the surface of a copper chaperone such as CopZ (Fig. 9) (70). Experiments in our lab have examined the mechanism of interaction betweens CopA and CopZ in *A. fulgidus* based upon the complementary protein surfaces (68). The LpCopA and CopZ from *E. hirae* crystal structures were used as a basis to create homology models and electrostatic maps, both of which predict a thermodynamically favorable interaction between $Cu^+ \bullet CopZ$ and CopA ($\Delta G = -11.11$ kcal/mol) (70). Additionally, when the positive docking site residues are replaced with nonpolar alanine residues, $Cu^+ \bullet CopZ$ is no longer able to transfer Cu^+ to CopA, even though the enzyme can still accept free Cu^+ from the media *in vitro* and the enzyme's turnover is not affected (68).

Another parameter explored in these experiments was the specific mechanism of Cu^+ transfer between $Cu^+ \bullet CopZ$ and CopA (68). The crystal structure of LpCopA confirms that M, D, and E residues conserved in Cu^+-ATPases are located close to the CopZ docking site (69). These residues are all capable of binding Cu^+ ions from the chaperone, and also in a position to transfer to the adjacent conserved CPC in TM 6, which along with conserved M and S residues in TM 8, comprise the two high-affinity TM-MBS, located near the periplasmic Cu^+ exit site (69). At this time, it is unclear whether Cu^+ is released freely to the periplasm or transferred directly to a periplasmic chaperone. Proper assembly of certain cuproteins, such as Cox, depends upon the presence of a functional Cu^+-ATPase (60, 71). This fact, coupled with the need to protect periplasmic proteins from the ROS generated in the presence of Cu^+, suggests that Cu^+ is likely transferred directly to a periplasmic partner.

1.2.5 Physiological roles of Cu^+-ATPases in symbiotic/pathogenic bacteria

The role of P_{1B}-ATPases in metal homeostasis is well established in eukaryotes (55, 72). Although all drive the efflux of heavy metals from the cytoplasm, their overall impact depends on subcellular localization and tissue distribution. For instance, in humans, there are two Cu^+-ATPases: hATP7A and hATP7B. Mutation of hATP7A, which is expressed in the basolateral membrane of intestinal epithelial cells, produces a copper

deficiency resulting in Menkes disease. Alternatively, mutation of hATP7B, expressed in liver cells, results in a decrease in excreted copper and causes Wilson's disease.

Physiological studies of P_{1B}-ATPases in bacteria and archaea suggest that the major role of these enzymes is to drive the efflux of substrate cations out of the cell as a mechanism to maintain intracellular heavy metal homeostasis (26, 44, 73). However, these studies have been mostly limited to gene deletion experiments testing the ability of these enzymes to confer resistance to increased levels of metals in the media. Bioinformatics analysis of bacterial genomes has shown numerous genes coding for P_{1B}-ATPases in symbiotic/pathogenic bacteria, many of which have the same metal specificity (1). This phenomenon is particularly noticeable in the case of the Cu^+-ATPases, with bacterial genomes often carrying up to five copies (40). If these enzymes were only involved in maintenance of cytoplasmic levels, there would be no need for multiple copies of these genes; thus, the presence of multiple ATPases with the same metal specificity is highly suggestive of each having a unique physiological role.

1.2.6 CopA1 and CopA2/FixI-like ATPases

In *Pseudomonas aeruginosa*, there are two homologous Cu^+-ATPases, CopA1 and CopA2, each having distinct cellular functions (60). CopA1 is the archetypical Cu^+-ATPase, having a well-characterized role in controlling cytoplasmic Cu^+ levels (26, 44, 74). Mutations in CopA1 lead to predictable phenotypes, including inability to grow in media containing increased copper and accumulation of Cu^+ in the cytoplasm (26-29). CopA2 appears structurally similar to CopA1, exhibiting the same membrane topologies, conserved N-MBD, and identical residues comprising the TM-MBSs. The main difference between these two enzymes is their respective transport kinetics (60). The CopA1 enzyme has a significantly higher $K_{1/2}$ and turnover rate than CopA2 ($K_{1/2}$=152.6 ± 7.9 µM and V_{max} = 63.1 ± 1.5 nmol mg^{-1} h^{-1} and $K_{1/2}$ = 20.7 ± 3.7 µM and V_{max}= 6.7 ± 0.4 nmol mg^{-1} h^{-1}, respectively) (60). This difference in relative activities can be attributed to the very different functions of these enzymes *in vivo* (61). Since CopA1 is responsible for clearance of potentially toxic Cu^+ ions, it must be able to transport Cu^+ out of the cell relatively quickly. CopA2, however, functions to metallate cytochrome *c* oxidase, and so has a lower turnover number.

Another indication that CopA1 and CopA2 are not redundant in function is the unique genetic environment of each. Like most Cu^+-ATPases, the *P. aeruginosa* CopA1 is translated in an operon that also includes a Cu^+ chaperone and a MerR-like TF having an extreme sensitivity to free Cu^+ in the cytoplasm (10^{-21} M) (20, 26, 27). In contrast, the *copA2* operon does not contain a MerR-like TF and is not induced by increase Cu^+ levels, but rather is located immediately downstream of an operon encoding cytochrome *c* oxidase (60). The *P. aeruginosa copA2* mutant does not have a Cu^+-sensitive phenotype of the *copA1* mutant, but does exhibit increased H_2O_2 sensitivity and decreased oxidase activity (60). Perhaps the strongest evidence that CopA1 and CopA2 each have a unique function *in vivo* is the inability of either CopA enzyme to complement the other, even when expressed under each other's promoter (i.e., *copA2* cannot complement the *copA1* mutant, even when expressed under the *copA1* promoter) (60).

1.3 The Rhizobia-legume symbiosis

Legumes, such as soybeans and peanuts, are the second-most widely harvested crop in the world (www.fao.org). Because of their high protein content, legumes are significant food sources for both humans and animals. In addition to foodstuffs, soybean oil is used in a variety of industrial products, including inks, biofuels, and paints. Legumes are also important due to their ability to replenish bioavailable nitrogen in the soil, reducing the need for fertilizers (75). The ability of leguminous plants to replenish nitrogen in the soil is derived from their symbiotic relationship with Rhizobiaceae bacteria. This mutualistic interaction results in formation of a novel plant organ, the root nodule. Here, the plant provides the bacteria with reduced carbon sources in exchange for nitrogen fixed by the bacteria. Crop rotation with leguminous plants such as alfalfa rather than nitrogen-containing fertilizers saves US farmers over $200 million per year (76). Thus, understanding the mechanisms enabling an effective symbiosis is both scientifically and economically relevant. In our lab, we use the model system of *Sinorhizobium meliloti* and its symbiotic partner, *Medicago sativa* (alfalfa), to study this process.

In the *S. meliloti-M.sativa* symbiosis, the process of nodulation can be divided into three main stages: pre-infection, nodule biogenesis, and differentiation. During the pre-infection stage, the rhizobia secrete nodulation (Nod) factors (77). These Nod factors are host-specific glycolipids that interact with receptors on the plant root hair membrane.

The presence of these Nod factors induces root hair curling, which traps the rhizobia inside the root hair. Nod factors also stimulate cortical cell division in the plant host, generating what will become the nodule primordia, and it the first step in nodule biogenesis (78). Once the rhizobium has been trapped inside the root hair, it stimulates localized degradation of the plant cell wall and depolarization of the plant plasma membrane (79). Depolarization is followed by an invagination of the plant plasma membrane, which becomes the plant-derived tubular structure known as the infection thread (IT) (78). The IT is filled with dividing bacteria, which grows toward the nodule primordium. Once an IT reaches the nodule primordium, plant cells form the meristem, and the infection thread continues to grow and branch behind it. Eventually, the rhizobia are taken up into the plant host cell via endocytosis (80). They are enveloped in a plant-derived membrane, and the bacteria stop dividing and begin to differentiate into bacteroids. This structure, known as the symbiosome, is the site of N_2 fixation in the nodule.

It is important to note that, although the relationship between rhizobia and legumes is mutualistic one, the initial process of nodulation begins with the rhizobial infection of plant host cells. As such, when infection thread formation begins, the plant cell responds by initiating a series of defense mechanisms known as the hypersensitive response (81). Also known as the oxidative burst, this response is characterized by the production of ROS, reactive nitrogen species (RNS), accumulation of phenolic compounds, and controlled plant cell apoptosis to limit pathogen progression in the host (82-84). ROS are also essential for efficient establishment and growth of the nodule primordia, elongation of the infection threads, nodule maturation, and senescence (85-88). For successful nodulation, rhizobia must be able to survive these challenges presented by the host cell. To accomplish this, rhizobia express periplasmic and membrane-bound metalloenzymes, such as catalases, SOD, and Cox. While some of these proteins are exported already folded in the holo (metallated) form via the Tat pathway, many are secreted unfolded via the Sec pathway and must acquire their metal cofactors in the

Figure 8: Zones of a mature indeterminate root nodule.

periplasm (2, 89).

Once bacteroid differentiation begins, the nodule begins to grow and elongate, resulting in an organ with clearly defined zones (Fig. 8) (90). Nodule growth takes place at its apical meristem (Zone I), which is a plant-derived process. The infection zone (Zone II) is the area in which bacteria are actually released into the plant cytosol to infect new cells. An intermediate zone (Zone II-III) is characterized by an accumulation of amyloplasts (starch-filled plastids) and is the area in which bacteria differentiate into bacteroids. The N_2 fixation zone (Zone III) consists mostly of plant cells infected with bacteroids, but also includes non-infected plant cells that take up the fixed nitrogen, mostly in the form of asparagine and glutamate (91). The senescent zone (Zone IV) is the zone closest to the root, and is the site of degradation of dying plant cells and bacteroids.

The functionality of the symbiosome is dependent on the ability of bacteroids to effectively couple N_2 fixation and carbon metabolism. Nitrogen fixation is achieved by the bacterial nitrogenase complex, which consists of two metalloprotein subunits localized to the cytoplasm (92). The overall reaction catalyzed by nitrogenase is $N_2 + 8H^+ + 16$ MgATP $+ 8e^- \rightarrow 2NH_3 + H_2 + 16$ MgADP $+ 16$ Pi. The mechanism of this reaction is outside the scope of this thesis and will not be discussed; for review, please see (93).

The function of nitrogenase is dependent on [Fe-S] clusters, and as such is inactivated, often irreversibly, when exposed to high levels of O_2 (94). Conversely, because N_2 fixation is such a high-energy process, requiring 16 ATP for every N_2 molecule fixed, ATP must be generated at high levels, which requires aerobic respiration via the tricarboxylic acid (TCA) cycle and oxidative phosphorylation. Thus, O_2 levels in the nodule must be tightly maintained so that the tension is low enough to prevent disruption of [Fe-S] of nitrogenase, but high enough that bacteroids are able to generate enough ATP. The problem of maintenance of proper oxygen levels is the plant's responsibility, and two main strategies are used to solve this conundrum (95). First, the plant protein leghemoglobin (Lb), which has a sub-micromolar affinity for oxygen ($K_m \sim$ 0.01 µM) is produced at high levels in the nodule (96). Secondly, localized changes in the inner cortex and the nodule interface prevent O_2 from diffusing into the nodule.

1.3.1 P_{1B}-ATPases in *Sinorhizobium meliloti*

The *S. meliloti* genome encodes eight P_{1B}-ATPases, many of which are localized to the symbiotic plasmids pSymA and pSymB (97, 98). These include five Cu^+-ATPases, a K^+-ATPase, a Zn^{2+}-ATPase, a Ni^{2+}/Fe^{2+}-ATPase, and one ATPase of unknown substrate (99, 100). The presence of multiple ATPases in rhizobia is not surprising, given that recent work has elucidated the importance of ATPases in bacterial virulence (101, 102). In order to survive the host hypersensitive response during establishment of symbiosis, rhizobia must secrete metalloenzymes, many of which acquire their metal cofactors in the periplasm. Due to their high redox potential and strong participation in Fenton chemistry, heavy metals are handled via protein-protein interactions, rather than simple diffusion through the periplasm. The specific mechanism(s) of heavy metal delivery to apo-proteins in the periplasm are yet unknown. It is easy to speculate a role for some of these ATPases in delivery of required metal cofactors to these proteins in the periplasm. It has already been demonstrated that P_{1B}-ATPases are required for *cbb$_3$*-Cox in a number of different species (60, 103, 104). In addition, our lab has recently reported that a P_{1B-5}-ATPase, CtpC, is responsible for loading Mn^{2+} to a secreted SOD in *M. smegmatis* (59). Thus, it is highly likely that some of the P-ATPases in the *S. meliloti* genome are also functioning to load metals to periplasmic apo-proteins, either directly or through a periplasmic partner.

Table 2: The five Cu^+-ATPases of *S. meliloti*. Homolgy to LpCopA was determined using BLAST

ATPase	Length	Gene	Homology to LpCopA
ActP	826 aa	Sma1013	46%
FixI1	757 aa	Sma1209	32%
FixI2	755 aa	Sma0621	50%
ActP2	827 aa	Smb21578	46%
CopA3	733 aa	Sma1087	46%

Of the five Cu^+-ATPases in the *S. meliloti* genome (Table 2), ActP has been

proposed to be the CopA1-like ATPase. It is expressed in an operon with a MerR-like TF, and has been shown to function in controlling cytoplasmic Cu^+ levels (100). FixI1 appears to be a CopA2-like protein, and its association with cbb_3-Cox assembly in other species has been well established (60, 103, 104). The $fixI1$ operon in most species is regulated by the FixLJ two-component regulatory system, which is activated by reduced O_2 tensions (105, 106). The FixI2 protein is located downstream of another putative cbb_3 Cox operon. However, neither FixI2 nor its associated Cox seem to be induced under microaerobic conditions (106).

No putative function has been assigned to ActP2; though it has a similar genetic environment to $actP$, it is not upregulated in response to Cu^+ under aerobic conditions, and the $actP2$ mutant does not accumulate Cu^+ (Patel et al, data not published). The $copA3$ gene has a unique genetic environment from the other Cu^+-ATPases, and the other genes in its putative operon have not been described. Mutation of CopA3 does not result in accumulation of Cu^+ or sensitivity to Cu^+ in the media; rather, the $copA3$ mutant has a significant decrease in Cu,Zn-SOD activity (Patel et al, data not published).

1.4 The role of Cu^+-ATPases in Cox assembly

The heme-copper respiratory oxidase (HCO) family includes a wide variety of bacterial and eukaryotic membrane enzyme complexes that act as the terminal electron acceptors in the electron transport chain of cellular respiration (107). There are great variations in the HCO family, but regardless of subtype of substrate, all HCOs ultimately function to catalyze the reduction of molecular O_2 to water. The free energy provided by this four-electron reduction allows a subunit(s) of the HCO to pump protons across the membrane, either to the periplasm (bacterial HCOs) or to the mitochondrial intermembrane space (eukaryotic HCOs). This proton gradient is then used as the driving force for oxidative phosphorylation by ATP synthase, and is thus responsible for the majority of ATP production during aerobic growth. In bacteria, there are many Cox proteins that are differentially expressed in response to varying O_2 levels in the environment. Chief amongst these are the aa_3-type, which is expressed under aerobic growth, and the cbb_3-type, which is prevalent under microaerobic growth conditions (108). Both types have at least one Cu^+ cofactor.

Studies on the biogenesis of bacterial Cox have been performed extensively in *Rhodobacter capsulatus* and *Bradyrhizobium japonicum* (104, 109, 110). In both cases, CcoI (FixI) have been shown to be essential for active cbb_3-formation. This Cox-deficient phenotype is also present in the *P. aeruginosa copA2* mutant (60). In all three cases, the phenotype is rescued by the addition of exogenous Cu^+ to the media. In these Cox proteins, the only Cu^+ cofactor present is in the ubiquitous subunit I. Interestingly, both of these species contain only FixI-type Cu^+-ATPase; however, deletions in *ccoI* do not appear to affect aa_3-Cox formation or activity in either *R. capsulatus* or *B. japonicum,* indicating that CcoI is responsible for Cu^+ delivery to the subunit I of the *cbb3*-Cox only (104, 110). Thus, it appears that different maturation proteins are responsible for functional assembly of the two different types of Cox proteins in these species. CoxG (also called CtgA), which is a homolog of the human Cox11, has been shown in *B. japonicum* to be essential for delivery of Cu^+ to the aa_3-Cox Cu_B site, but not to the cbb_3 Cu_B site (111). ScoI (alco called SenC or PrrC, appears to be responsible for delivery of Cu^+ to the Cu_A site in subunit II of the aa_3-Cox, as well as the Cu_B site in the *R. capsulatus* cbb_3-Cox (112). Both of these chaperones are anchored to the membrane and localized to the periplasmic side/intermembrane space (113). A third periplasmic protein involved in Cu^+ delivery in some species has been described. This protein, termed PCu, is a soluble protein that is thought to accept Cu^+ from SenC and deliver it to CcoN/FixN (114). To date there have been no reports describing the mechanisms of Cox assembly in *S. meliloti.* However*,* bioinformatics analysis shows that homologs of all three chaperones are present in the *S. meliloti* genome (see Results).

1.5 FixI1 and FixI2

Interestingly, the genome of *S. meliloti* encodes not one but two FixI-type Cu^+-ATPases. Like *fixI1*, the *fixI2* gene is located immediately downstream of a putative cbb_3-
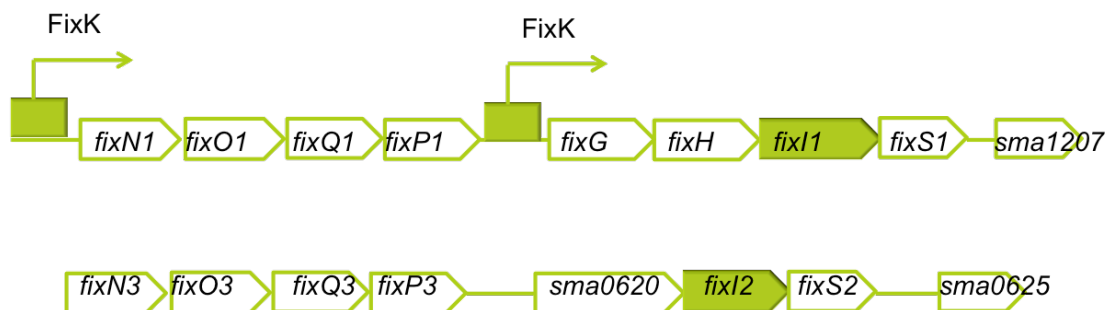

Figure 9: Genetic environments of fixI1 and fixI2. Both operons are downstream of putative cbb3-type cytochrome c oxidase operons. FixK binding sites appear upstream of both fixN1 and fixG, suggesting these genes are upregulated under microaerobic conditions.

Cox (Fig. 9). Both the *fixNOQP1* and *fixGHIS1* operons have been demonstrated in other rhizobial species to be under the regulation of FixK, a TF associated with the FixLJ two-component regulatory system, an O_2-sensitive regulatory system that induces genes important during microaerobic growth of *S. meliloti* (105). In many, but not all, of these species, the Cox and ATPase operons are co-transcribed as one transcript (60, 108). In *S. meliloti,* both operons have an upstream FixK binding site, suggesting that they may be transcribed separately in this species.

In the case of the *fixNOQP3* and *fixI2* operons, bioinformatics analysis of the promoter regions show that they lack both classical and non-canonical FixK binding sites, and microarray data shows that neither of these operons is induced under microaerobic growth conditions (106). This differential gene expression pattern, combined with the unique phenotypes associated with each *fixI* mutant, suggests that each is performing a distinct physiological function during the legume-rhizobia symbiosis. **Given that the stresses a rhizobium encounters change during the different stages of infection and nodulation, I hypothesize that both FixI1 and FixI2 have distinct, non-redundant functional roles during different stages of the nodulation process, and that each is responsible for Cu^+ loading different periplasmic chaperones. In turn, these two different copper chaperones metallate two distinct Cox proteins, which have different physiological roles.** Towards testing this hypothesis, the work described within this thesis demonstrates that *S. meliloti* strains carrying mutations in either *fixI1* or *fixI2* generates a distinct phenotype *in planta;* that neither FixI1 nor FixI2 are responsible for maintenance of cytoplasmic Cu^+ levels; and that mutation of *fixI1* and *fixI2* results in different respiratory-deficient phenotypes.

2. Materials and methods

2.1 Bacterial strains and culture conditions

A library of signature-tagged insertional mutants of *S. meliloti* has been described (115). Briefly, the gene is interrupted by a transposon insertion that disrupts the coding region of the gene without introducing a frameshift mutation. *S. meliloti* 2011 (wild-type, WT) and the *fixI1* transposon mutant carrying an mTn5 transposon insert containing a neomycin resistance marker (*fixI1::mTn5*) were obtained from Dr. Jacques Batut (University of Tolouse, France). A mutant strain carrying the same mTn5 transposon insertion in *fixI2* (*fixI2::mTn5*) were obtained from Dr. Anke Becker (Center for Biotechnology, University of Bielefeld, Germany) (115). *S. meliloti wild-type strain* WSM419 and the *actP* insertional mutant (*actP::*mTn5) were obtained from Dr. Wayne Reeve (Murdoch University, Australia) (100). All strains were grown in TY liquid media (0.5% tryptone, 0.3% yeast extract, 0.09% CaCl$_2$) and supplemented with 200 μg/mL streptomycin (WT), 100 ug/mL neomycin (*fixI1::mTn5* and *fixI2::mTn5*), or 20 μg/mL chloramphenicol (WSM419 and *actP::mTn5*) as appropriate. Strains were generally grown shaking at 180 rpm at 30°C for 36 h.

2.2 Insertional mutation analysis

Polymerase chain reaction (94°C for 2 min initially, followed by 30 cycles of 94°C for 30 s, 55°C for 60 s, and 72°C for 90 s, with a final 7 min extension cycle at 72°C) was

used to verify that the transposon insertion was present in the mT5n strains. WT *fixI1* was amplified using primers 5'Sma1209 and 3'Sma1209, which sit at the 5' and 3' ends of the *fixI1* gene and
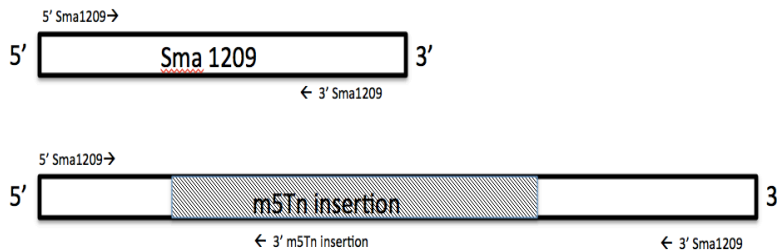
Figure 11: PCR design. In the top example, the primers would amplify full-length *fixI1*, yielding an amplicon of 2,271 bp. In the bottom example, if the mTn5 insertion is present, the primers would amplify a region of 1,615 bp.

amplify the entire gene (Fig. 11). WT *fixI2* was amplified using primers 5'Sma0621 and 3'Sma0621, which amplify the entire gene. Transposon insertional mutants were verified using either 5'Sma1209 (for *fixI1::mTn5* insertion) or 5'Sma0621 (for *fixI2::mTn5* insertion) and 3'mTn5insert, which amplifies 268 bp of the mTn5 insertion. This insertion is located at 1347 bp in *fixI1* (expected mutant amplicon = 1615 bp) and at 1670 in *fixI2*

(expected mutant amplicon = 1938 bp). PCR products were separated by electrophoresis in a 1% agarose gel and visualized with 0.1 µL/mL ethidium bromide.

2.3 Nodulation profiles and plant growth analysis

M. sativa (alfalfa) seeds were surface sterilized by submerging them in 100% ethanol for 30 s, followed by 5 min in 15% bleach and 5 washes with sterile Milli-Q water. Seeds were incubated in the dark at 4°C overnight on moistened cotton in sterile petri plates. Seeds were germinated in the sterile petri dishes for 48 h in the dark at room temperature before planting. Seedlings were planted in glass tubes filled with an agar slant of modified, nitrogen-free Murashige and Skoog medium containing 0.5 mL/L of Plant Solutions A (2 M $CaCl_2 \bullet 2\ H_2O$), B (2.2 M K_2HPO_4, 350 mM KH_2PO_4), C (25 mM $FeC_6H_6O_7$), and D (0.5 M $MgSO_4 \bullet H_2O$, 0.5 M K_2SO_4, 2 mM $MnSO_4 \bullet H_2O$, 0.8 mM $ZnSO_4 \bullet 7\ H_2O$, 3 mM H_3BO_3, 0.4 mM $CuSO_4 \bullet 5\ H_2O$, 50 µM $CoSO_4 \bullet 7\ H_2O$, and 0.1 mM $Na_2MoO_4 \bullet 2\ H_2O$), pH 6.6-6.9. Plant roots were covered by foil and grown at 24°C, 16 h light/8 h dark cycle with light intensity of 250 µmol m s^{-1}. Roots of three-day-old seedlings were inoculated by direct application of 1.5 mL of bacterial cultures at OD = 1.5 to the root and observed daily until emergence of first nodule. Number of nodules was recorded at 10, 20 and 30 days post infection (dpi). Nodule size and color relative to WT-infected plants were noted and excised from the root and photographed at various time points. For plant growth experiments, plants were harvested after 20 dpi, root and shoot separated, and dried to a constant weight at 80°C.

2.4 Viable counts

Seeds were sterilized, planted and inoculated as previously described. At 20 dpi, all nodules were excised from roots, washed five times with sterile Milli-Q water, and crushed in 1 mL sterile TY media. Serial dilutions were plated in triplicate on yeast extract-mannitol agar (YEMA) plates containing Congo Red (116). Plates were incubated at 30°C for 5 days before counting colonies. Data were normalized to total number of nodules collected per plant to determine number of colony forming units (CFUs) per nodule.

2.5 Nodule light microscopy

Nodules were excised from plants 20 dpi and fixed in a mixture of 4% paraformaldehyde, 0.25% glutaraldehyde, 2.5% sucrose in 50 mM potassium phosphate buffer, pH 7.4 at 4 °C for 24 h (117). Nodules were dehydrated through an ethanol series (0, 30, 50, 70, 85, 90, 95, 100%) and embedded in LR White resin (London Resin Company, UK) in gelatin capsules. Thin sections (0.7-1.0 μm) were obtained with a Leica EM UC6 ultramicrotome (Leica Microsystems, Wetzlar, Germany). Sections were then stained with 1% osmium tetroxide and counter-stained with 0.1% toluidine blue. Microscopic observations were performed in a ZEISS Axioscope optical microscope (Carl Zeiss, Germany).

2.6 Copper accumulation analysis

Copper accumulation analysis was performed as described previously with minor modifications (60). *S. meliloti* WT 2011, WSM 419, *actP::mTn5*, *fixI1::mTn5,* and *fixI2::mTn5* were grown as described to late exponential phase (OD =1.5-1.8). For Cu^+ challenge, medium was supplemented with 0.15 mM $CuSO_4$ and cells incubated at 30°C for 1 h. After incubation, cells were harvested, washed with 0.9% NaCl, and pellets resuspended in 200 μL Milli-Q water. A 100 μL aliquot was used to measure total protein content by the Bradford method (118). The other 100 μL aliquot was acid digested with 300 μL HNO_3 (trace metal grade) for 1 h at 80°C, then overnight at room temperature. Digest was completed with addition of 30% H_2O_2, and samples brought to a final volume of 3 mL. Cu^+ content was measured by atomic absorption spectroscopy (AAS) (AAnalyst 300, Perkin-Elmer, Foster City, CA, USA). Standards used were 8, 16, and 32 μg/L Cu^+, giving a linear concentration range from 1-50 μg/L.

2.7 Oxidase activity assays

Membrane fractions from 250 mL cultures of *S. meliloti* wild type and mutant strains were prepared as previously described with minor modifications (53). Briefly, cells were grown as described above and harvested at OD =1. Pellets were washed with ice cold buffer containing 50 mM 4-(2-hydroxyethyl)-1-piperazineethanesulfonic acid (HEPES), 200 mM NaCl and then resuspended in 25 mL 50 mM HEPES, 200 mM NaCl, 1 mM phenylmethansulfonyl fluoride (PMSF). Cells were lysed by three passages through a French press at 20,000 psi. Lysed cells were centrifuged at 8,000 *x g* for 30

min to remove intact cells and cell walls. Membranes were recovered from the supernatant by centrifugation at 100,000 x g for 1 h. Membranes were resuspended in 1 mL 50 mM HEPES, 200 mM NaCl, 1 mM PMSF, homogenized and stored at -20°C. Oxidase activity was measured as previously described by González-Guerrero et al. with minor modifications (60). Assays were performed in a final volume of 1.1 mL 50 mM HEPES, 200 mM NaCl. The reaction was initiated by the addition of 5 μL 0.54 M N,N,N',N'-tetramethyl-p-phenylenediamine (TMPD). Oxidase activity was monitored at 563 nm and normalized to total protein as measured by Bradford (118).

2.8 Bioinformatics analysis of potential cytoplasmic and periplasmic chaperones of FixI1 and FixI2

To identify potential cytoplasmic copper chaperones of FixI1 and/FixI2, a BLAST search was conducted using the protein sequence of *E. hirae* CopZ (1CPZ) from PubMed as a target sequence (119). PubMed searches for SenC and CtaG homologs in the *S. meliloti* genome yielded three protein hits. In addition, a BLAST search for a potential third periplasmic chaperone, PCu$_A$P, recently implicated in Cox assembly in certain species was performed using *Deinococcus radiodurans* (1X9L) as a template (114, 120).

3. Results and Discussion

3.1 Verification of rhizobia insertional mutations

PCR analysis of WT and mutant rhizobia cells confirmed that full-length *fixI1* (2,271 bp) and *fixI2* (2,265 bp) were not present in the respective insertional mutant strains (Fig. 12, lanes 2A and 4A). Though a band similar in size to *fixI1* was amplified in the *fixI1::mTn5* strain, this band is due to nonspecific amplification. This same band was not present in WT DNA when reacted with the same primers (Fig. 12, lane 1B), nor was any band detected in the *fixI1* mutant DNA when reacted with full-length *fixI1* primers (Fig. 12, lane 2A). The reverse primer for the mutant strain (3'-mTn5_insert) was designed to amplify 268 bp of the transposon insertion, resulting in expected amplicon sizes of 1615 bp for the *fixI* mutant and 1,938 bp for the *fixI2* mutant (Fig. 12). As expected, the mutant amplicons are present only when mutant, not WT, DNA is amplified.
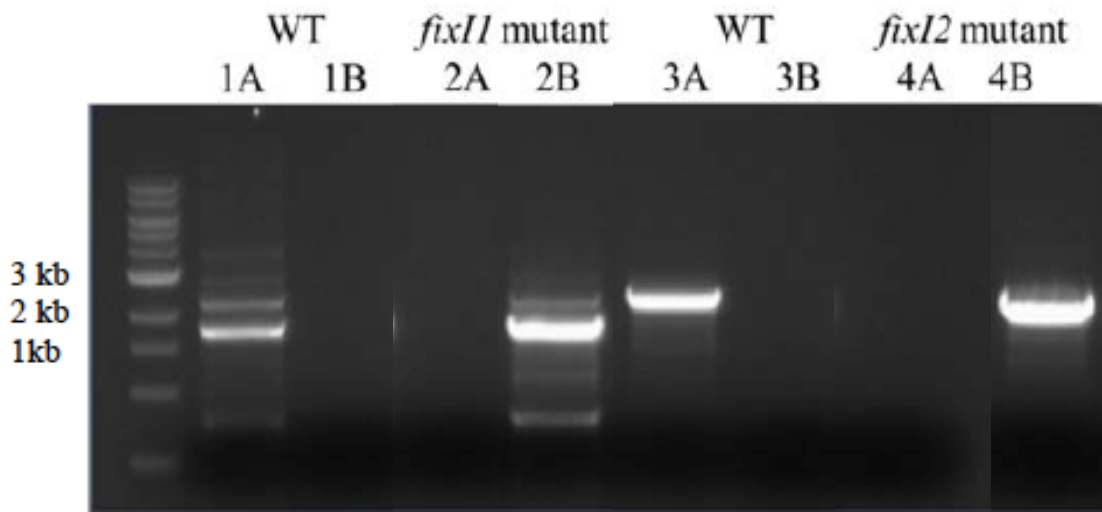
Figure 12: Confirmation of rhizobia insertional mutants. DNA from indicated strains was amplified with primers designed to amplify either full length fixI1 (1A, 2A) or fixI2 (3A, 4A) or designed to amplify the 5' region of fixI1and a portion of the m5Tn transposon insertion (1B, 2B) or the 5' region of fixI2 and a portion of the m5Tn transposon insertion (3B, 4B).

3.2 Mutations in *fixI1* and *fixI2* result in distinct phenotypes *in planta*

The first question addressed in this project was how the lack of functional FixI1 and FixI2 proteins affected the rhizobial interaction with alfalfa. Since both of these genes are located on the symbiotic plasmid pSymA, it is reasonable to speculate that

they play some role during symbiosis. By infecting *M. sativa* seedlings with WT or mutant strains, and tracking their growth, it is possible to observe the effect of *fixl1* and *fixl2* mutation on many aspects of this process. These included appearance of first nodule, number of nodules formed, color, size, and morphology of nodules, and overall plant health, as compared to plants infected with the WT strain.
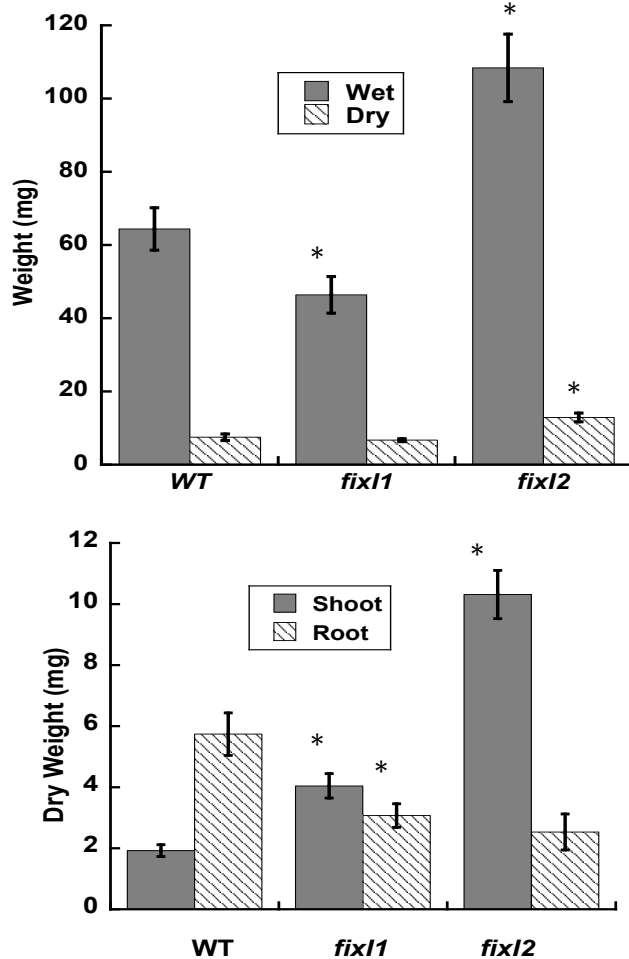
Figure 13: Mutations in *fixl1* and *fixl2* result in growth changes after 20 days post-infection (dpi). Top panel: Total wet weight (solid) and dry (hashed) weights. Lower panel: Comparison of dry shoot (solid) and root (hashed). Data are reported as the mean ± SE, n=10. * indicates p ≤ 0.05.

Mutations in both *fixl1* and *fixl2* affected plant growth when compared to those infected by WT *S. meliloti*. Plants infected with the *fixl1* mutant were impaired in growth, both in the roots and shoots (Fig. 13, top panel). The plants infected with the *fixl2* mutant did not appear to have problems with growth, and had both a higher wet and dry weight than the plants infected by WT *S. meliloti* (Fig. 13, lower panel). Interestingly, despite the smaller shoots observed in plants infected with the *fixl1* mutant (Fig. 14), the shoots of both *fixl1* and *fixl2*-mutant derived plants had a significantly higher dry weight than that of plants infected with WT rhizobia. However, upon comparison of the dry weights of the roots and shoots, it was observed that both the *fixl1* and *fixl2* mutation resulted in a decrease in root dry weight. This decrease was significant only in plants infected with the *fixl1* mutant, and this lower biomass could be indicative of reduced N_2-fixation (121). It is clear that these rhizobial mutations both result in altered plant growth; however, these experiments are not sufficient to explain why these growth patterns were observed.

31

3.2 Effect of *fixl1* and *fixl2* mutation on nodulation profiles

Considering the importance of nodules on plant growth, the effect of *fixi1* and *fixl2* mutation on nodule formation was analyzed. Compared to plants infected with the WT, the *fixl1* mutant-infected plants showed a significant delay in first nodule appearance (Table 3). This suggested that the *fixl1* mutant is more susceptible to the host immune response at some point during the initial infection process. This was in contrast with the *fixl2* mutant-infected plants, which formed nodules at the same rate as the WT-infected plants (Table 3). Comparison of the number of nodules formed by each strain at 10 versus 30 dpi, however, showed that both the WT and *fixl1* mutant strains continued to generate more nodules over time (Fig. 14).

Interestingly, although the *fixl2* mutant-infected plants generated more nodules initially, there was no significant increase in total number of nodules from 10 to 30 dpi (Fig. 14). The plant can control nodule formation, and will prevent new nodules from forming and/or cause

Figure 14: Effect of fixl1 and fixl2 mutation on nodulation profiles. (a) 14 plants were infected with WT, fixl1 mutant or fixl2 mutant rhizobia and observed daily for first nodule emergence.
(b) Comparison of number of nodules at 10 days post infection (dpi) and 30 dpi. n = 14. Data are represented as the mean ± SE, n=10. * indicates p< 0.05.

S. meliloti strain	Days post infection
WT2011	5.2 ± 0.5
fixl1::mTn5	7.13 ± 0.03*
fixl2::mTn5	5.7 ± 0.6

Table 3: Appearance of first nodule
* indicates p< 0.05

early nodule senescence if N_2-fixation is not happening at a sufficient rate (121). Thus, the lack of new nodule formation over time in plants infected with the *fixl2* mutant suggested that this mutant has no problem surviving the initial infection process, but rather is deficient in its ability to establish an effective symbiosis once in the nodule. Additionally, the increase in number of nodules in the *fixl2* mutant-infected plants at 10 dpi suggested that the plant initially generates more nodules in an attempt to compensate for the lack of nodule functionality (Fig. 14). These two opposite phenotypes
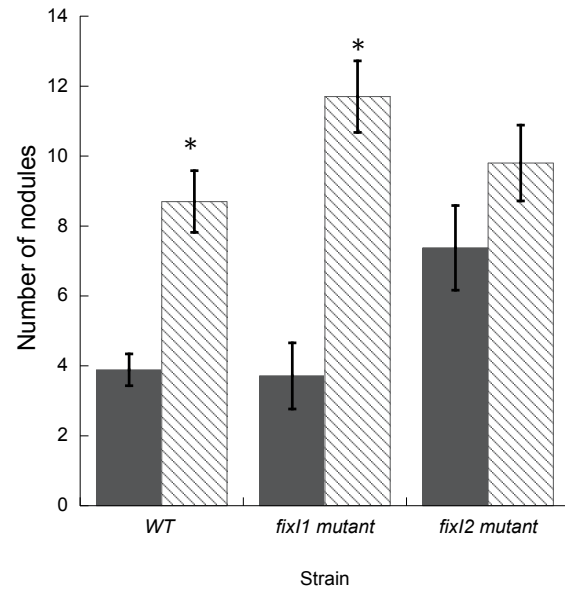
further supports the idea that FixI1 and FixI2 have very different cellular roles and are each important at varying times during nodulation.

3.3 Effect of *fixI1* and *fixI2* mutation on nodule viable counts

The indeterminate nodule contains two different populations of rhizobia: undifferentiated, free-living bacteria, and differentiated, N_2-fixing bacteroids. In species that form indeterminate nodules, such as *S. meliloti*, bacteroids are not able to reproduce, nor are they capable of reverting back to the undifferentiated bacteria (122). Thus, if nodules are collected, crushed to release bacteria/bacteroids, and grown on agar plates, only undifferentiated bacteria will grow. Nodules induced
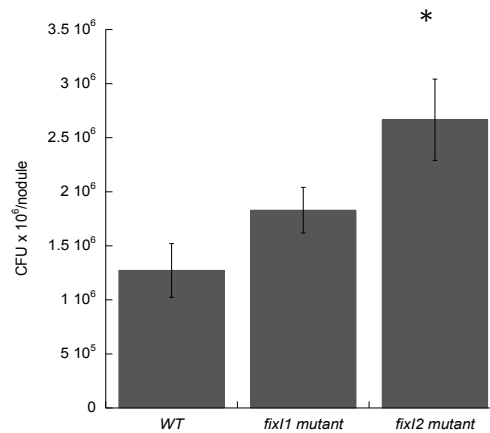
Figure 15: Viable counts from nodules infected with WT, fixI1 or fixI2 mutant. Nodules were collected at 20 dpi. Data are reported as mean ± SE, n =5. * indicates p< 0.05

by the *fixI2* mutant strain had higher viable counts than either the WT or the *fixI1* mutant infected plants (Fig. 15), indicating that there were a significantly greater number of bacteria per *fixI2*-infected nodule. This most likely corresponded to a decreased number of differentiated bacteroids, supporting the hypothesis that the *fixI2* mutant has difficulty differentiating into bacteroids in the nodule.

3.4 Effect of *fixI1* and *fixI2* mutation on zone formation in nodules

Nodules derived from both the *fixI1* and *fixI2* mutant strains showed differences in morphology from those derived from WT rhizobia strains. These differences were examined more closely via light microscopy on semi-thin sections, to see if there were any observable differences in zone formation in mature nodules (Fig. 9). Very little difference was noted in the size and proportion of infected (IC, yellow arrows) versus uninfected cells (UIC, blue arrows) in the *fixI1* mutant nodules when compared to the WT-derived nodules (Fig. 16). This result was not surprising, since phenotypically, the *fixI1* mutant has difficulties forming nodules, not maintaining them. The *fixI2* mutant-

derived nodules, however, had much larger senescent zones (Fig. 16C, red arrows), which are composed primarily of dead bacteroid cells to be degraded by the plant. These data, along with the increase in viable bacteria counts from *fixI12*-mutant derived nodules, supports the hypothesis that the *fixI2* mutant phenotype results in an impaired ability of *fixI2* mutant rhizobia to successfully differentiate into bacteroids in the nodule.
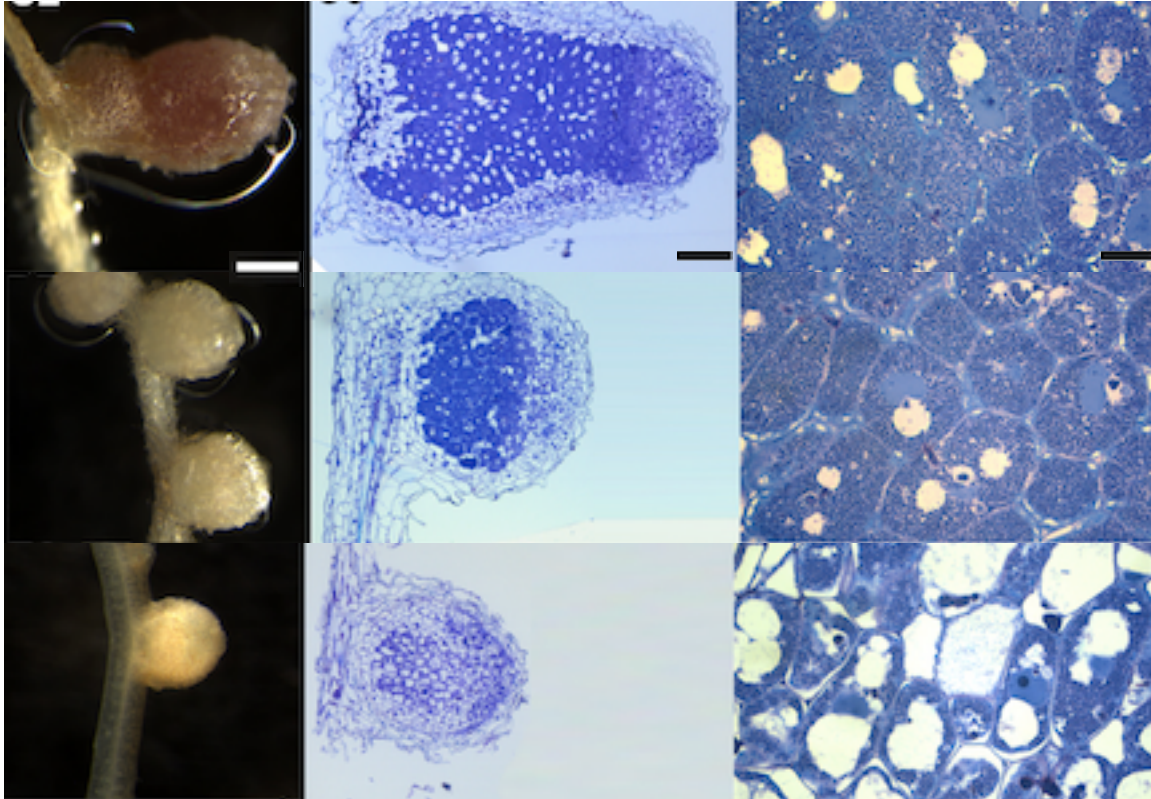
Figure 16: Morphological and histological analysis of 21 dpi *M. sativa* nodules induced by *Sinorhizobium* wild type (top panel), *fixI1* mutant (middle panel) and *fixI2* mutant (bottom panel) strains. (1) Macroscopic nodule morphology, bars = 500 µm; (2) semi-thin longitudinal nodule sections, bars = 150 µm; (3) magnification of the nodule N_2 fixation region (zone III); bars = 20 µm. The *fixI2* mutant derived nodules show a substantial decrease in bacteroids (dark blue staining) and much larger senescent zone than either the wild-type or *fixI1*-type derived nodules.

3.5 Effect of *fixI1* and *fixI2* on whole cell Cu$^+$ accumulation and Cu$^+$ sensitivity under aerobic growth

Both *fixI1* and *fixI2* have the classical hallmarks of Cu$^+$-ATPases: CPC in TM 6, NYG in TM7, and MXSS in TM 8. ActP has already been suggested to be the detoxifying enzyme in *S. meliloti* (100), a phenotype that has been confirmed by our lab (Patel *et al*, data not published). Therefore, if either FixI1 or FixI2 are acting to keep intracellular Cu$^+$ levels low, cells lacking functional enzyme are expected to exhibit Cu$^+$ sensitivity and accumulate Cu$^+$ in a manner similar to the *actP* mutant. Using the *actP* mutant and its parental strain WSM 418 as controls, strains were grown both in non-supplemented media and in media supplemented with CuSO$_4$, and cell growth and whole cell Cu$^+$ content were measured.
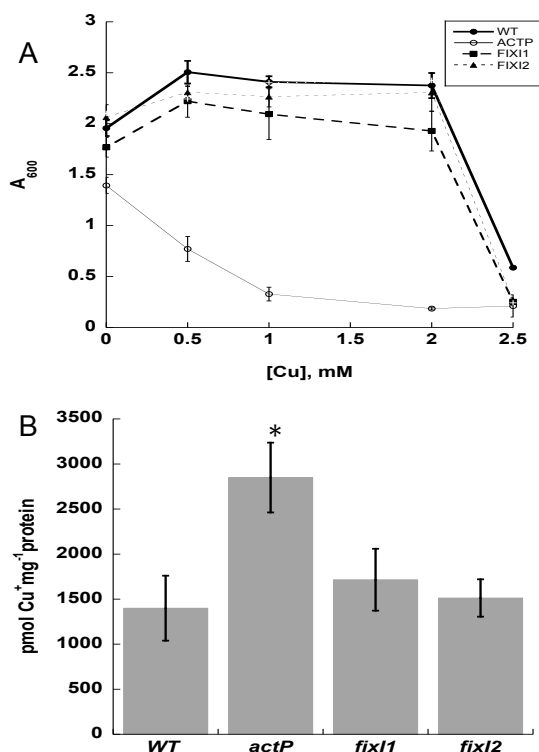
Figure 17: ActP is the only Cu$^+$-ATPase responsible for intra-cellular Cu$^+$ levels. A: Growth of WT (•), fixI1 mutant (■), fixI2 mutant (▲), WSM 418 (◊) and actP mutant (○) in response to increasing Cu$^+$ concentrations. B: Cu$^+$ levels measured in the same strains after challenge with 0.15 mM CuSO$_4$ and normalized to mg total cell protein.
Data represents the mean ± SE, n =3, * indicates p < 0.05

Neither *fixI1* nor *fixI2* mutants exhibited any significant increase in Cu$^+$ sensitivity compared to the WT (Fig. 17A), Neither mutant accumulate Cu$^+$, even when grown in media containing 1.5 mM CuSO$_4$ (Fig. 17B). This was in sharp contrast to the *actP* mutant, the traditional CopA-like ATPase. Together, these experiments demonstrated that neither FixI1 nor FixI2 were responsible for keeping intracellular copper low, and indicates that they both likely play some other physiological role in rhizobia.

3.5 Effect of *fixI1* and *fixI2* mutations in oxidase activity

Considering that *S. meliloti* lives in both aerobic (in the free-living form) and microaerobic (during infection and in nodule) environments, it is tempting to speculate
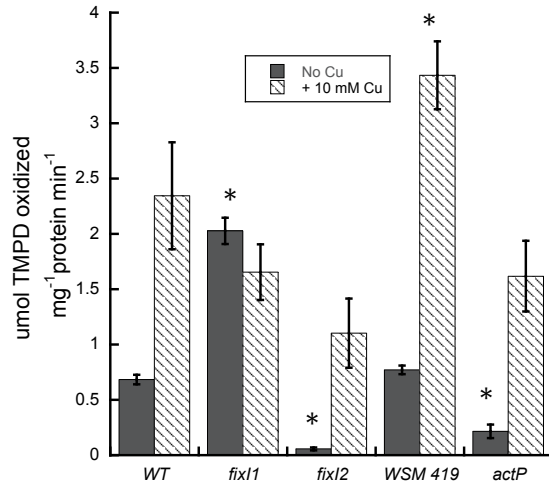
Figure 18: Mutation in *fixI2* causes a respiratory-deficient phenotype in aerobically grown cells. Data are represented as the mean ± SE , n = 5. *indicates p < 0.05.

that FixI1 and FixI2 are responsible for maturation of two different Cox assemblies expressed under different oxygen conditions. Given the presence of a FixK both upstream of the *fixI1* operon, it was hypothesized that FixI1 was important for respiration under low oxygen tensions. When cells were grown aerobically and oxidase activity was measured, there was a significant decrease in the *fixI2* mutant strains (Fig. 19, black bars), suggesting that this ATPase metallates a Cox responsible for aerobic respiration. Interestingly, a decrease in Cox activity was also observed in the *actP* mutant (Fig. 19, black bars). Initially it was thought that this decrease might be due to a disruption of [Fe-S] clusters in strains lacking functional ActP, as this is a common mechanism of Cu^+ toxicity (10). However, since *actP* mutants do not accumulate Cu^+ when grown in non-supplemented media (data not shown), this is unlikely the reason for the respiratory defect. However, the WSM 419 strain not only accumulated a significantly lower amount of Cu^+ when grown in media containing 0.15 mM $CuSO_4$ than the WT 2011 strain (Fig. 16), but the WSM 419 wild-type also had a significantly higher increase in Cox activity when grown in the presence of 10 µM Cu (Fig. 18, white bars). Although these strains are closely related, there may be slight differences in their biology that makes the WSM proteins, and thus those of the ActP mutant, more sensitive to the presence of Cu.

Interestingly, aerobically grown *fixI1* mutant cells actually had a higher level of oxidase activity when compared to the WT. In some species, such as *Pseudomonas*, there are two *cbb₃*-Cox (123). Expression of the first Cox is thought to regulate a variety of other genes under limited oxygen, and its presence represses the expression of another respiratory complex. It is tempting to speculate a similar role for *fixNOQP1* in rhizobia, especially considering the presence of a third *fixNOQP2* operon on pSymA, which is not associated with any ATPase (97).

It is well documented that respiratory-deficient phenotypes due to non-functioning Cu^+-ATPases can be rescued by the addition of micromolar amounts Cu^+ to the media (60, 103). As expected, this phenotype was rescued with the addition of exogenous Cu^{2+} to the media. However, an increase in oxidase activity was noted in all strains, except the *fixI1* mutant, when 10 µM Cu^{2+} was added to the media. Although it exhibited no increase in activity, the *fixI1* mutant had oxidase activity comparable to the WT (Fig. 19, gray bars). Thus, from this experiment, it was unclear whether the increased activity in the presence of Cu^+ is due to a rescue of the Cox-deficient phenotype or to the presence of Cu^+ itself.

3.6 Identification of potential cytoplasmic and periplasmic partners of FixI1 and FixI2

To identify potential cytoplasmic copper chaperones of FixI1 and/FixI2, a BLAST search was conducted using the protein sequence of *E. hirae* CopZ (1CPZ) as a target sequence. BLAST results gave two non-ATPase hits with low E values: NP_437079.7 (Smb20560) and NP_435791.2 (Sma1009). The presence of Sma1009 directly upstream of ActP (Sma1013), the classical Cu^+-ATPase, suggests that its gene product is the cytoplasmic partner of ActP. Given that FixI1 and FixI2 are directing Cu^+ to a particular protein target, it is reasonable that there is a second cytoplasmic chaperone responsible for directing Cu^+ to the appropriate ATPase.

Two membrane-tethered proteins have already been identified as Cox assembly proteins in multiple species. SenC, also called ScoI or PrrC, has been associated with delivery of Cu^+ to the Cu_B site (subunit 1) of the *cbb₃*-type Cox in *R. capsulatus* (112). In *S. meliloti,* this gene is chromosomally encoded at locus Smc01471. CtaG, a Cox11 homolog, has been demonstrated to be essential for Cu^+ to the *aa₃*-type, but not the *cbb₃*-type Cox (111). A homolog has already been identified in PubMed as a putative Cox assembly protein (NP_385014.1, Smc00012). A third soluble periplasmic protein, PCu_AP, has been implicated in *aa₃*-type Cox assembly in *D. radiodurans* (120). Protein BLAST returned one hit (E=4.0 x 10^{-6}), a putative signal peptide (NP_385656, Smc01242). Given the association each has in other species with *aa₃*-type Cox assembly, I hypothesize that both of these periplasmic chaperones are interacting with FixI2 and participating in the assembly of a constitutively expressed Cox.

4. Conclusions

The presence of two copies of genes encoding for Cu^+-ATPases is a common phenomenon amongst pathogenic/symbiotic bacteria. These two homologous proteins can be divided into two distinct subfamilies: CopA-like and FixI-like Cu^+-ATPases (60). In species such as *P. aeruginosa,* these two proteins have been shown to be non-redundant, with each having a unique genetic environment and physiological role. Less common are bacterial genomes that contain three or more copies of Cu^+-ATPases, as occurs in certain rhizobium species such as *S. meliloti.* We hypothesized that the presence of multiple FixI-type ATPases was not an example of redundancy, but rather an evolutionary adaptation that allowed rhizobia to survive under the wide variety of adverse conditions faced during early infection and establishment of symbiosis. Towards this goal, this work focused on examining the effects of mutation of each ATPase on both free-living bacteria and on the ability of rhizobia to establish an effective symbiosis with its host legume.

The first objective was to confirm that neither FixI1 nor FixI2 had physiological roles as CopA-type detoxifying proteins. Thus, each mutant strain was tested for Cu^+ sensitivity and accumulation. As expected, neither gene mutation resulted in the hallmark Cu^+-sensitive phenotype of CopA mutation when grown in media supplemented with $CuSO_4$. However, this was most likely a secondary effect due to lack of functional cytochrome *c* oxidase, and thus an inability to mediate ROS generated by excess Cu^+ in the cytoplasm. This result was further supported by the lack of Cu^+ accumulation in either *fixI1* or *fixI2* mutant strains.

Next the effect of *fixI1* and *fix2* mutation on symbiosis with legumes was examined. The *fixI1* mutant showed a significant delay in development of nodules; however, once nodules began to form, there was no difference in nodule development when compared to plants inoculated with the WT strain. This phenotype suggested that this mutation significantly affected the ability of *S. meliloti* to establish infection threads. The *fixI2* mutant exhibited no delay in nodule formation; however, it failed to continue to generate new nodules, suggesting that the nodules formed by this mutant might be ineffective. This hypothesis was supported by increased bacterial counts from crushed nodules and changes in morphology of nodule sections.

Finally, the effect of *fixI1* and *fixI2* mutation of oxidase activity was measured. It was hypothesized that *fixI2* is a constitutively expressed gene, and that its associated Cox was responsible for aerobic respiration. This hypothesis was supported by the

observation that in aerobically grown cells, the *fixI2* mutant, but not the *fixI1* mutant, is respiratory-deficient. Preliminary experiments were performed to assay the affect of *fixI1* and *fixI2* mutation on respiratory activity under microaerobic conditions. Under microaerobic growth, only the *fixI1* mutant showed a respiratory-deficient phenotype, suggesting that this ATPase provides Cu^+ to a Cox important for respiration under low O_2. These results were supported by gene expression experiments performed in our lab, which showed that *fixI1* is induced during microaerobic growth and in the presence of nitrosative stressors. In contrast *fixI2* expression levels remain constant in all conditions tested, suggesting it is constitutively expressed (Patel et al, in preparation). It is clear that FixI2 is playing some role in symbiosis, due to its altered phenotype during nodule maturation (See Fig. 15b and Fig 16). However, taking the data together, it appears that the Cox activity associated with FixI2 is important during the metabolic switch that accompanies bacteroid differentiation, rather than for respiration of the bacteroids in nodules. Conversely, the *fixI1* mutant exhibited a decrease in oxidase activity only when cells were grown in microoxic conditions. These results confirmed that, from a physiological standpoint, these two enzymes are not functionally redundant *in vivo*.

Future experiments in this project may include both assaying ATPase activity in the presence of various cytoplasmic and periplasmic chaperones, as well as modeling electrostatic interactions between FixI1, FixI2, and the putative partner proteins. These experiments may further elucidate whether the differences reported here are strictly the result of transcriptional control, or if mechanistic differences exist in their specific protein-protein interactions when transporting Cu^+ from the cytosol to the periplasmic face of the membrane-bound Cox.

REFERENCES

1.   Argüello JM (2003) Identification of ion selectivity determinants in heavy metal transport P1$_B$-type ATPases. *J Membr Biol* **195,** 93-108

2.   Waldron KJ and Robinson NJ (2009) How do bacterial cells ensure that metalloproteins get the correct metal? *Microbiology* **7**, 25-35

3.   Fraustro de Silva JJR and Williams RJP (2001) *The Biological Chemistry of the Elements*, 2nd ed., Oxford University Press, New York

4.   Keen CL and Gershwin ME (1990) Zinc deficiency and immune function. *Annu Rev Nutr* **10**, 415-431

5.   Percival S (1998) Copper and immunity. *Am J Clin Nutr* **67**, 1064S-1068S

6.   Jaiser SR and Winston GP (2010) Copper deficiency myelopathy. *J Neurol* **257,** 869-881

7.   Stohs SJ and Bagchi D (1995) Oxidative mechanisms in the toxicity of metal ions. *Free Radic Biology Med* **18**, 321-336

8.   Prousek J (2007) Fenton chemistry in biology and medicine. *Pure Appl Chem* **79**, 2325-2338

9.   Stadtman ER (1993) Oxidation of free amino acid residues in proteins by radiolysis and metal-catalyzed reactions. *Annu Rev Biochem* **62**, 797-821

10.   Macomber L and Imlay JA (2009) The iron-sulfur clusters of dehydratases are primary intracellular targets of copper toxicity. *Proc Natl Acad Sci U S A* **106**, 8344-8349

11.   Rutherford JC and Bird AJ (2004) Metal-Responsive Transcription factors that Regulate Iron, Zinc, and Copper Homeostasis in Eukaryotic Cells. *Eukaryotic Cell* **3**, 1-13

12.   Rensing C and Grass G (2003) *Escherichia coli* mechanisms of copper homeostasis in a changing environment. *FEMS Microbiology Reviews* **27**, 197-213

13.   Rae TD, Schmidt PJ, Pufahl RA, Culotta VC, and O'Halloran TV (1999) Undetectable intracellular free copper: The requirement of a copper chaperone for superoxide dismutase. *Science* **284**, 805-808

14.   Palmgren MG and Nissen P (2011) P-type ATPases. *Annu Rev Biophys* **40**, 243-266

15.   Nies DH (2003) Efflux-mediated heavy metal resistance in prokaryotes. *FEMS Microbiol Rev* **27**, 313-339

16.   Brown NL, Stoyanov JV, Kidd SP, and Hobman JL. (2003) The MerR family of transcriptional regulators. *FEMS Microbiol Rev* **27**, 145-163

17.   Liu T, Ramesh A, Ma Z, Ward SK, Zhang L, George GN, Talaat AM, Sacchettini JC, and Giedroc DP.(2007) CsoR is a novel *Mycobacterium tuberculosis* copper-sensing transcriptional regulator. *Nat Chem Biolo* **3**, 60-68

18.   Brocklehurst KR, Hobman JL, Lawley B, Blank L, Marshall SJ, Brown NL, and Morby AP (1999) ZntR is a Zn(II)-responsive MerR-like transcriptional regulator of *zntA* in *Escherichia coli*. *Mol Microbiol* **31**, 893-902

19.   Solioz M and Stoyanov JV (2003) Copper homeostasis in *Enterococcus hirae*. *FEMS Microbiol Rev* **27**, 184-195

20.   Changela A, Chen K, Xue Y, Holschen J, Outten, CE, O'Halloran TV, and Mondragón (2003) Molecular basis of metal-ion selectivity and zeptomolar senstivitity by CueR. *Science* **301**, 1383-1387

21.   Outten FW, Outten CE, Hale JA, and O'Halloran TV. (2000) Transcriptional activation of an *Escherichia coli* copper efflux regulon by the chromosomal MerR homologue, cueR. *J Biol Chem* **275**, 31024-31029

22. Lee SM, Grass G, Rensing C, Barret SR, Yates CJD, Stoyanov, JV and Brown NL (2002) The Pco proteins are involved in periplasmic copper handling in *Escherichia coli*. *Biochem Biophys Res Commun* **295**, 616-620

23. Outten FW, Huffman DL, Hale JA, and O'Halloran TV. (2001) The independent *cue* and *cus* systems confer copper tolerance during aerobic and anaerobic growth in *Escherichia coli*. *J Biol Chem* **276,** 30670-30677

24. Hernandez-Montes G, Argüello JM, and Valderrama B. (2012) Evolution and diversity of periplasmic proteins involved in copper homeostasis in gamma bacteria. *BMC Microbiology* **12**, 249-263.

25. Grass G and Rensing C (2001) CueO is a multi-copper oxidase that confers copper tolerance in *Biochem Biophys Res Commun* **286**, 902-908

26. Osman D and Cavet JS (2008) Copper homeostasis in bacteria. *Adv Appl Microbiol* **65**, 217-247

27. Solioz M, Abicht HK, Mermod M and Mancini S (2010) Response of Gram-negative bacteria in response to stress. *J. Biol. Inorg Chem* **15**, 3-14

28. Schwan WR, Warrener P, Keunz E, Stover CK, and Folger KR (2005) Mutations in the *cueA* gene encoding a copper homeostasis P-type ATPase reduce the pathogenicity of *Pseudomonas aeruginosa* in mice. *Int J Med Microbiol* **295**, 237-242

29. Teitzel GM, Geddie A, De Long SK, Kirisits MJ, Whiteley M, and Parsek MR (2006) Survival and Growth in the Presence of Elevated Copper: Transcriptional Profiling of Copper-Stressed *Pseudomonas aeruginosa*. *J Bacteriol* **188**, 7242-7256

30. Roberts SA, Weichsel A, Grass G, Thakali K, Hazzard JT, Tollin G, Rensing C, and Montfort WR (2002) Crystal structure and electron transfer kinetics of CueO,

a multicopper oxidase required for copper homeostasis in *Escherichia coli*. *Proc Natl Acad Sci U S A* **99**, 2766-2771

31. Berks BC, Sargent F, and Palmer T (2000) The Tat protein export pathway. *Mol Microbiol* **35**, 260-274

32. Mana-Capelli S, Mandal A, and Argüello JM. (2003) *Archeglobus fulgidus* CopB is a thermophilic Cu^{2+}-ATPase-Functional role of its histidine-rich N-terminal metal binding domain *J Biol Chem* **278**, 40534-40541

33. Tetaz TJ and Luke RK (1983) Plasmid-controlled resistance to copper in *Escherichia coli*. *J Bacteriol* **154**, 1263-1268

34. Rouch DA and Brown NL (1997) Copper-inducible transcriptional regulation at two promoters in the *Escherichia coli* copper resistance determinant pco. *Microbiol* **143**, 1191-1202

35. Munson GP, Lamb DL, Outeen FW, and O'Halloran TV (2000) Identification of a copper-responsive two-component system on the chromosome of *Escherichia coli* K-12. *J Bacteriol* **182**, 5864-5871

36. Franke S, Grass G, Rensing C, and Nies DH (2003) Molecular analysis of the cpper-transporting efflux system CusCFBA of *Escherichia coli*. *J Bacteriol* **185**, 3804-3812

37. Kim EH, Nies DH, McEvoy MM, and Rensing C (2011) Switch or funnel: How RND-Type transport systems control periplasmic metal homeostasis. *J Bacteriol* **193**, 2381-2387

38. Bagai I, Rensing C, Blackburn NJ and McEvoy MM (2008) Direct metal transfer between periplasmic proteins identifies a bacterial copper chaperone. *Biochemistry* **47**, 11408-11414

39. Hood I and Skaar EP (2012) Nutritional immunity: transition metals at the pathogen-host interface. *Nat Rev Microbiol* **10**, 525-537

40. Argüello JM, González-Guerrero M and Raimunda D (2011) Bacterial Transition Metal ATPases:Transport Mechanisms and Roles in Virulence. *Biochemistry* **50**, 9940-9949

41. White C, Lee J, Kambe T, Fritsche K, and Petris MJ. (2009) A role for the ATP7A copper-transporting ATPase in macrophage bactericidal activity. *J Biol Chem* **284**, 33949-33956

42. Wagner D, Maiser J, Lai B, Cai Z, Barry CE 3rd, Honer Zu, Bentrup K, Russell DG, and Bermudez LE (2005) Elemental analysis of *Mycobacterium avium*-, *Mycobacterium tuberculosis*-, and *Mycobacterium smegmatis*-containing phagosomes indicates pathogen-induced microenvironments within the host cell's endosomal system *J Immunol* **174**, 1491-1500

43. Albers RW (1967) Biochemical aspects of active transport. *Annu Rev Biochem* **36**, 727-756

44. Argüello JM, Eren E, and González-Guerrero M (2007) The structure and function of heavy metal transport P_{1B}-ATPases. *Biometals* **20**, 233-248

45. Axelsen KB and Palmgren MG (1998) Evolution of substrate specificities in the P-Type ATPase superfamily. *J Mol Evol* **46**, 84-101

46. Paulusma CC and Elferink RP (2010) P4 ATPases--the physiological relevance of lipid flipping transporters. *FEBS Letters* **584**, 2708-2716

47. Lutsenko S, Petrukhin K, Cooper MJ, Gilliam CT, and Kaplan JH (1997) N-terminal domains of human copper-transporting adenosine triphosphatases (the Wilson's and Menkes disease proteins) bind copper selectively in vivo and in vitro with stoichiometry of one copper. *J Biol Chem* **272**, 18939-18944

48. Eren E, Kennedy DC, Maroney MJ, and Argüello JM. (2006) A novel regulatory metal binding domain is present in the C terminus of Arabidopsis Zn^{2+}-ATPase HMA2. *J Biol Chem* **281**, 33881-33891

49.   Tsivkovskii R, MacArthur BC, and Lutsenko S (2001) The Lys 1010-Lys 1325 fragment of the Wilson's disease protein binds nucleotides and interacts with the N-terminal domain of this protein in a copper-dependent manner *J Biol Chem* **276**, 2234-2242

50.   Mandal AK and Argüello JM (2003) Functional roles of metal binding domains of the *Archaeoglobus fulgidus* Cu$^+$-ATPase CopA. *Biochemistry* **42**, 11040-11047

51.   Takahashi M, Kondou Y, and Toyoshima C. (2007) Interdomain communication in calcium pump as revealed in the crystal structures with transmembrane inhibitors. *Proc Natl Acad Sci USA* **104**, 5800-5805

52.   Hilge M, Siegal G, Vuister GW, Guntert P, Gloor SM, and Abrahams JP (2003) ATP-induced confromational changes of the nucleotide-binding domain of Na,K-ATPase. *Nat Struct Biol* **10**, 468-474

53.   Mandal AK, Cheung WD and Argüello JM (2002) Characterization of a thermophilic P-type Ag$^+$/Cu$^+$-ATPase from the extremophile *Archaeoglobus fulgidus*. *J Biol Chem* **277**, 7201-7208

54.   Sharma R, Rensing C, Rosen BP, and Mitra B. (2000) The ATP hydrolytic activity of purified ZntA, A Pb(II)/Cd(II)/Zn(II)-translocating ATPase from *Escherichia coli J Biol Chem* **275**, 3873-3878

55.   Eren E and Argüello, JM (2004) Arabidopsis HMA2, a divalent heavy-metal-transporting P$_{1B}$-type ATPase, in involved in cytoplasmic Zn^{2+} homeostasis. *Plant Physiol* **136**, 3712-3723

56.   Scherer J and Nies DH (2009) CzcP is a novel efflux system contributing to transition metal reisitance in *Cupriavidus mettallidurans* CH34. *Mol Microbiol* **73**, 601-621

57.   Seigneurin-Berny D, Gravot A, Auroy P, Mazard C, Kraut A, Finazzi G, Grunwald D, Rappaport F, Vavasseur A, Joyard J, Richaud P and Rolland N (2006) HMA1

a new Cu-ATPase of the Chloroplast envelope, is essential for growth under adverse light conditions. *J Biol Chem* **281**, 2882-2892

58.   Raimunda D, Long J, Sasetti CM, and Argüello JM (2012) Role in metal homeostasis of CtpD, a Co^{2+}-transporting P_{1B4}-ATPase of *Mycobacterium smegmatis*. *Mol Microbiol* **84**, 1139-1149

59.   Padilla-Benavides T, Long J, Raimunda D, Sassetti CM, and Argüello JM. (2013) CtpC, a novel P_{1B}-type Mn^{2+}-transporting ATPase is required for secreted protein metallation in mycobacteria. *J Biol Chem* **288**, 11334-11347

60.   González-Guerrero M, Raimunda D, Cheng X, and Argüello JM (2010) Distinct functional roles of homologous Cu^+ efflux ATPases in Pseudomonas aeruginosa. *Mol Microbiol* **78**, 1246-1258

61.   Raimunda D, González-Guerrero M, Leeber BWIII and Argüello JM (2011) The transport mechanism of bacterial Cu^+-ATPases: distinct efflux rates adapted to different function. *Biometals* **24**, 467-475

62.   Raimunda D, Subramanian P, Stemmler, T and Argüello JM (2012) Tetrahedral coordination of zinc during transmembrane transport by P-type Zn^{2+}-ATPases. *Biochem Biophys Acta* **1818**, 1374-1377

63.   Holm RH, Kennepohl P and Solomon E (1996) Structural and functional aspects of metal sites in biology. *Chem Rev* **96**, 2239-2314

64.   Traverso ME, Subramanian P, Davydov R, Hoffman BM, Stemmler TL, and Rosenwieg AC (2010) Identification of a hemerythin-like domain in a P_{1B}-type transport ATPase. *Biochemistry* **49**, 7060-7068

65.   Post RL, Hegyvary C, and Kume S (1972) Activation by adenosine triphosphate in the phosphorylation kinectics of sodium and potassium ion transport adenosine triphosphatase. *J Biol Chem* **247**, 6530-6540

66.   Kühlbrandt W (2004) Biology, structure, and mechanism of P-ATPases. *Nat Rev Mol Cell Biol* **5**, 282-295

67.   González-Guerrero M and Argüello JM (2008) Mechanism of Cu^+-transporting ATPases: Soluble Cu^+ chaperones directly transfer Cu^+ to transmembrane transport sites. *Proc Natl Acad Sci USA* **105**, 5992-5997

68.   Padilla-Benevidas T, McCann, CJ, and Argüello, JM (2012) Mechanism of Cu^+-transporting ATPases: Soluble Cu^+ chaperones directly transfer Cu^+ and the role of transient metal binding sites. *J Biol Chem* **288**, 69-78

69.   Gourdon P, Liu XY, Skyørringe T, Morth JP, Møller JP, Pederson BP and Nissen P (2011) Crystal structure of a copper-transporting P_{1B}-type ATPase. *Nature* **475**, 59-64

70.   Argüello JM, Raimunda, D and González-Guerrero M (2012) Metal transport across membranes: emerging models for a distinct chemistry. *J Biol Chem* **287**, 13510-13517

71.   Preisig, O., Zufferey, R., and Hennecke, H. (1996) The Bradyrhizobium japonicum fixGHIS genes are required for the formation of the high-affinity cbb3-type cytochrome oxidase. *Archives of Microbiology* **165**, 297-305

72.   Lutsenko S, Barnes NL, Bartee MY, and Dmitriev OV. (2007) Function and regulation of human copper-transporting ATPases. *Physiol Rev* **87**, 1011-1046

73.   Rensing C, Fan B, Sharma R, Mitra B, and Rosen BP. (2000) CopA: An *Escherichia coli* Cu(I)-translocating P-type ATPase. *Proc Natl Acad Sci USA* 97, 652-656

74.   Solioz M, Abicht HK, Mermod M and Mancini S. (2010) Response of Gram-negative bacteria in response to stress. *J Biol Inorg Chem* **15**, 3-14

75.   Graham PH and Vance CP (2003) Legumes: Importance and Constraints to Greater Use. *Plant Physiology* **131**, 872-877

76. Peterson TA and Ruselle MP (1991) Alfalfa and the nitrogen cycle in the corn belt. *J Soil Water Conserv* **46**, 229-235

77. Eckardt NA (2006) The Role of Flavanoids in Root Nodule Development and Auxin Transport in *Medicago Truncatula*. *Plant Cell* **18**, 1539-1540

78. Gage DJ (2004) Infection and invasion of roots by symbiotic, nitrogen-fixing rhizobia during nodulation of temperate legumes. *Microbiol Mol Biol Rev* **68**, 280-300

79. Sutton JM, Lea EJA, and Downie JA (1994) The Nodulation-Signaling Protein NodO from *Rhizobium leguminosarum* Biovar viciae Forms Ion Channels in Membranes. *Proc Natl Acad Sci USA* **91**, 9990-9994

80. Brewin NJ (2004) Plant cell wall remodelling in the rhizobia-legume symbiosis. *Crit Rev Plant Sci* **23**, 293-316

81. Santos R, Hérouart D, Sigaud S, Touati D, and Puppo A (2001) Oxidative Burst in Alfalfa-Sinorhizobium meliloti Symbiotic Interaction. *MPMI* **14**, 86-89

82. Hutzler P, Fischbach R, Heller W, Jungblut TP, Reuber S, Schmitz R, Veit M, Weissenbock G, Scnitzler JP (1998) Tissue localization of phenolic compounds in plants by confocal laser scanning microscopy. *J Exp Bot* **49**, 953-965

83. Delleddonne MPA and Murgia I (2003) The Functions of Nitric-Oxide Mediated Signalling and Changes in Gene Expression During the Hypersensitive Response. *Antioxid Redox Signalling* **5**, 33-41

84. Greenberg JT (1997) Programmed Cell Death in Plant-Pathogen Interactions. *Annu Rev Plant Physiol Plant Mol Biol* **48**, 525-545

85. Jamet A, Mandon K, Puppo A, and Herouart D (2001) H2O2 is required for optimal establishment of the *Medicago sativa*/*Sinorhizobium meliloti* symbiosis. *J Bacteriol* **189**, 8741-8745

86.   D'Haeze W, De Rycke R, Mathis R, Goormachtig S, Pagnotta S, Verplanke C, Capoen W, and Holsters M (2003) Reactive oxygen species and ethylene play a positive rols in lateral root base nodulation of a semiaquatic legume. *Proc Natl Acad Sci USA* **100**, 11789-11794

87.   Matamoros MA, Baird LM, Escuredo PR, Dalton DA, Minchin FR, Iturbe-Ormaetxe I, Rubio MC, Moran JF, Gordon AJ, and Becana M (1999) Stress-Induced Legume Root Nodule Senescence. Physiological, Biochemical, and Structural Alterations. *Plant Physiology* **121**, 97-112

88.   Alesandrini F, Mathis R, Van de Sype G, Herouart D, and Puppo A (2003) Possible roles for a cysteine protease and hydrogen peroxide in soybean nodule development and senescence. *New Phytologist* **158**, 131-138

89.   Tottey S, Waldron KJ, Firbank SJ, Reale B, Bessant C, Sato K, Cheek TR, Gray J, Banfield MJ, Dennison C, and Robinson NJ (2008) Protein-folding location can regulate manganese-binding versus copper- or zinc-binding. *Nature* **455**, 1138-1142

90.   Franssen HJ, Vijn I, Yang WC, and Bisseling T (1992) Developmental ascpects of the Rhizobium-legume symbiosis. *Plant Mol Bio* **19**, 89-107

91.   Udvardi MK and Day DA (1997) Metabolite transport across symbiotic membranes of legume nodules. *Annu Rev Plant Physiol Plant Mol Bio* **48**

92.   Planque K, Kennedy IR, de Vries GE, Quispel A, and van Brussel A (1977) Location of Nitrogenase and Ammonia-Assimilatory Enzymes in Bacteriods of *Rhizobium leguminosarum* and *Rhizobium lupini*. *J Gen Microbiol* **102**, 95-104

93.   Burgess BK and Lowe DJ (1996) Mechanism of Molybdenum Nitrogenase. *Chem Rev* **96**, 2983-3012

94.   Gallon JR (1981) The oxygen sensitivity of nitrogenase. *Trend Biochem Sci* **6**, 19-23

95. Crespi M and Galvez S (2000) Molecular mechanisms in root nodule development *J Plant Growth Regul* **19**, 155-166

96. Ott T (2005) Symbiotic leghemolglobins are crucial for nitrogen fixation in legume root nodules but not for general plant growth and development. *Curr Biol* **15**, 531-535

97. Barnett MJ, Jones T, Komp C, Abola AP, Barloy-Hubler F, Bowser L, Capela D, Galibert F, Gouzy J, Gurjal M, Hong A, Huizar L, Hyman RW, Kahn D, Kahn ML, Kalman S, Keating DH, Palm C, Peck MC, Surzycki R, Wells DH, Yeh KC, Davis RW, Federspiel NA, Long SR. (2001) Nucleotide sequence and predicted functions of the entire Sinorhizobium meliloti pSymA megaplasmid. *Proc Natl Acad Sci USA* **98**, 9883-9888

98. Finan TM, Weidner S, Wong K, Buhrmester J, Chain P, Vorhölter FJ, Hernandez-Lucas I, Becker A, Cowie A, Gouzy J, Golding B, Pühler A. (2001) The complete sequence of the 1,683-kb pSymB megaplasmid from the N2-fixing endosymbiont Sinorhizobium meliloti. *Proc Natl Acad Sci USA* **98**, 9889-9894

99. Zielazinski EL, González-Guerrero M, Subramanian P, Stemmler TL, Argüello JM and Rosenzweig AC (2013) Sinorhizobium meliloti Nia is a P1B-5-ATPase expressed in the nodule during plant symbiosis and is involved in Ni and Fe transport. *Metallomics* **5**, 1614-1623

100. Reeve WG, Tiwari RP, Kale NB, Dilworth MJ, and Glenn AR (2002) ActP controls copepr homeostasis in *Rhizobium legunimosarum* bv. *viciae* and *Sinorhizobium meliloti* preventing low pH-inducced copper toxicity. *Mol Microbiol* **43**, 981-991

101. Sasetti CM and Rubin EJ (2003) Genetic requirements for mycobacterial survival during infection. *Proc Natl Acad Sci USA* **100**, 12989-12994

103. Hassani BK, Astier C, Nitschke W, and Ouchane S (2010) CtpA, a copper-translocating P-type ATPase involved in the biogenesis of multiple copper-requiring enzymes. *J Biol Chem* **285**, 19330-19337

104. Koch HG, Winterstein C, Saribas AS, Alben JO and Daldal F(2000) Roles of the *ccoGHIS* gene products in the biogenesis of the *cbb₃*-type cytochrome c oxidase. *Journal of Molecular Biology* **297**, 49-65

105. Bobik C, Meilhoc E and Batut J (2006) FixJ: A major regulator of the oxygen limitation response and late symbiotic functions of *J Bacteriol* **188**, 4890-4902

106. Becker A, Berges H, Krol E, Bruand C, Ruberg S, Capela D, Lauber E, Meilhoc E, Ampe F, de Bruijn FJ, Fourment J, Francez-Charlot A, Kahn D, Kuster H, Liebe C, Puhler A, Weidner S, and Batut J (2004) Global changes in gene expression in Sinorhizobium meliloti1021 under micoroxic and symbiotic conditions. *MPMI* **17**, 292-303

107. Garcia-Horseman JA, Barquera B, Rumbley J, MA J and Gennis RB. (1994) The superfamily of heme-copper respiratory oxidases. *J Bacteriol* **176**, 5587-5600

108. Presig, O., Anthamatten, D. and Hennecke, H (1993) Genes for a novel, microaerobically induced oxidase complex in *Bradyrhizobium japonicum* are essential for a nitrogen-fixing symbiosis. *Proc. Natl. Acad. Sci. USA* **90**, 3309-3313

109. Kulajta, C., Thumfart, J. O., Haid, S., Daldal, F., and Koch, H.-G. (2006) Multi-step Assembly Pathway of the cbb3-type Cytochrome c Oxidase Complex. *Journal of Molecular Biology* **355**, 989-1004

110. Presig O, Zufferey R and Hennecke H (1996) The *Bradyrhizobium japonicum fixGHIS* genes are required for the formation of the high-affinity type *cbb3*-cytochrome *c* oxidase. *Archives of Microbiology* **165**, 297-305

111. Buhler, D., Rossman, R., Landolt, S., Balslger, S., Fischer, H., and Hennecke, H. (2010) Disparate Pathways for the Biogenesis of Cytochrome Oxidases in *Bradyrhizobium japonicum*. *Journal of Biological Chemistry* **285**, 15704-15713

112. Nittis T, George GN and Winge DR (2001) Yeast Sco1. *J Biol Chem* **276**, 42520-42526

113. Robinson NJ and Winge DR (2010) Copper chaperones. *Annu Rev Biochem* **79**, 537-562

114. Ekici S, Pawlik G, Lohmeyer E, Koch HG, Daldal F. (2012) Biogenesis of cbb(3)-type cytochrome c oxidase in Rhodobacter capsulatus. *Biochem Biophys Acta* **1817**, 898-910

115. Pobigaylo, N., Wetter, D., Szymczak, S., Schiller, U., Kurtz, S., Meyer, F., Nattkemper, T., and Becker, A. (2006) Construction of a Large Signature-Tagged Mini-Tn5 Transposon Library and Its Application to Mutagenesis of *Sinorhizobium meliloti*. *Applied and Envrionmental Microbiology* **72**, 4329-4337

116. Vincent J (1970) *A manual for the practical study of root nodule bacteria*, Blackwell Scientific Publications, Oxford

117. Rodriguez-Haas, B., Finney, L., Vogt, S., González-Melendi, P., Imperial, J. & González-Guerrero, M. . (2013) Iron distribution throught the developmental stages of *Medicago truncatula* nodules. *Metallomics: Integrated Biometal Science* **5**, 1247-1253

118. Bradford MM (1976) A rapid and sensitive method for th e. *Anal Biochem* **72**, 248-254

119. Wimmer RHT, Solioz M, and Wuthrich K (1999) NMR structure and metal interactions of the CopZ copper chaperone. *J Biol Chem* **274**, 22597-22603

120. Banci, L., Bertini, I., Ciofi-Baffoni, S., Katsari, E., Katsaros, N., Kubicek, K., and Mangani, S. (2005) A copper(I) protein possibly involved in the assembly of CuA

center of bacterial cytochrome c oxidase. *Proceedings of the National Academy of Sciences of the United States of America* **102**, 3994-3999

121.   Cohen E, Oken Y, Kigel J, Nur I, and Henis Y. (1980) Increase in dry weight and total nitrogen content in *Zea mays* and *Setaria italica* associated with nitrogen-fixing *Azospirillum* sp Plant *Physiology* **66**, 746-749

122.   Van de Velde W, *et al* (2010) Plant peptides govern terminal differentiation of bacteria in symbiosis. *Science* **327**, 1122-1126

123.   Comolli, JC and Donohue TJ. (2004) Differences in two *Pseudomonas aeruginosa cbb*$_3$ cytochrome oxidases. *Molecular Microbiology* **51**, 1193-1203

APPENDIX 1: List of primers used in this work

Primer Name	Sequence
5'-SMa1209	5'-ATGAGCTGCTGCGCCTCTAGT-3'
3'-SMa1209	5'-TGAGGTCACCGCGCCTGAAT-3'
5'-SMa0621	5'-ATGTCCTGCTGCTCTGGTATAGCCGT-3'
3'-SMa0621	5'-TATCTTTGCCGTGGCTGGTTT-3'
3'-mTn5 insert	5'-CTGACTCTTATACACAAGTG-3'